Title: Time-Restricted Feeding Extends Healthspan in Both Sexes and Lifespan in Male C57BL/6J Mice

Authors: Samantha E. Iiams[1 †], Nathan J. Skinner[1 †], Mary Wight-Carter[2], Victoria A. Acosta-Rodríguez[1,4*], Carla B. Green[1*], and Joseph S. Takahashi[1,3*]

Affiliations:
[1]Department of Neuroscience, Peter O'Donnell Jr. Brain Institute, University of Texas Southwestern Medical Center, Dallas, TX, USA
[2]Animal Resource Center, University of Texas Southwestern Medical Center, Dallas, TX, USA
[3]Howard Hughes Medical Institute, University of Texas Southwestern Medical Center, Dallas, TX, USA
[4]Present address: Circadian Biology of Aging Unit, Translational Gerontology Branch, National Institute on Aging (NIA/NIH), Baltimore, MD, 21224, USA

[†] These two authors contributed equally to this work and are co-first authors

[*] Corresponding authors:
Victoria A. Acosta- Rodríguez (VAR); victoria.acosta-rodriguez@nih.gov
Carla B. Green (CBG); carla.green@utsouthwestern.edu,
Joseph S. Takahashi (JST); joseph.takahashi@utsouthwestern.edu

Abstract: Time-restricted feeding (TRF) aligned with an organism's circadian rhythm has been shown to improve health, but its long-term effects on healthspan and lifespan in mammals, especially under normal dietary conditions, remain unclear. Here, we examined the impact of 12-hour (h) and 8h nightly TRF windows in male and female mice fed regular chow. TRF improved multiple health measures, including behavioral rhythmicity, body weight and composition, frailty, and disease onset. These effects were most pronounced in the 8h-TRF group, which exhibited voluntary caloric restriction in addition to time restriction. A composite Healthspan Index revealed that TRF extended healthspan in both sexes, though the benefits were more prolonged in females relative to their total lifespan. Median lifespan was significantly extended in males under 8h-TRF by 12%, whereas females showed no significant lifespan extension, highlighting sex-specific responses to TRF.

Main Text:

While human life expectancy has nearly doubled since the early 20th century (*1*), healthspan remains limited, with many spending over 10% of their lives in poor health due to age-related functional declines and disease development (*2*). Caloric restriction (CR), a potent aging intervention involving a 30-50% reduction in food intake without malnutrition, has been extensively studied for its ability to delay the onset of age-associated diseases, including cancer, cardiovascular disorders, and neurodegeneration, while extending lifespan across multiple model organisms (*3-5*). Incorporating daily feeding/fasting cycles with CR enhances these geroprotective effects (*6-9*), and aligning feeding with an organism's active circadian phase can further extend lifespan (*10*). This synergy likely reflects both the synchronization of nutrient intake with internal metabolic processes and the protective effects of temporal compartmentalization, driven by circadian clock-regulated gene expression in the liver and other peripheral tissues (*11-18*).

Aging triggers a progressive damping of circadian rhythmicity in both humans and animal models. This decline, evident in behavior and physiology, stems from a reduction in amplitude and shifted phases of the molecular clock's transcriptional output (*19*). Interventions that restore circadian rhythms can improve health and extend longevity in model organisms (*20*), suggesting that optimizing meal timing is a promising strategy to counteract age-related rhythm disruptions and promote healthy aging (*21*).

Given that CR is challenging to maintain in people (*22*), meal timing alone via time-restricted feeding (TRF) in animals, or time-restricted eating (TRE) in humans, has emerged as an alternative strategy to delay aging (*23, 24*). TRF, which restricts feeding to specific daily windows without limiting overall caloric intake, can confer similar benefits as timed CR, including improved rhythmic gene expression, cognitive function, and cardiometabolic health, even in obesity models

fed a high-fat, high-sucrose diet (*25-32*). Recent clinical TRE trials report high adherence and improved cardiometabolic outcomes in subjects with pre-existing conditions, demonstrating its potential as a feasible intervention to enhance human healthspan (*33-37*).

However, few studies have examined the benefits of TRF/TRE under typical metabolic conditions without diet- or genetically-induced obesity (*38-40*), and even fewer have compared impacts between the sexes (*41*). The long-term impact of TRF on healthspan and lifespan in mammalian models also remains unclear (*42, 43*). In this study, we sought to address these key knowledge gaps and determine whether TRF could serve as an effective aging intervention for healthy male and female mice.

Results:

Early Onset Circadian Aligned TRF Has Sex-Specific Impacts on Longitudinal Feeding and Wheel-Running Activity Levels

To determine how time-restricted feeding (TRF) impacts healthspan and lifespan in mammals, we individually housed 264 female and 264 male C57BL/6J mice in wheel cages with automated feeders at 2 months of age. To measure impacts under normal nutritional conditions, mice were fed purified precision pellets (Bioserv F0075). For the first 8-weeks, all mice were fed *ad libitum* (free-feeding; AL) with access to a maximum of 22 pellets or 6.6g (23.8 Kcal) per day. At 4 months of age, N=78/sex were switched to a 12-hour (h) TRF window (Zeitgeber time (ZT) 12-24) and another N=78/sex to an 8h-TRF window (ZT14-22) both circadian aligned to the night, the active phase of nocturnal rodents. The remaining N=108/sex were maintained AL to serve as the control. Across all feeding groups, mice were provided with a daily allotment of food that exceeded their

typical intake, and no group ever consumed the full amount, ensuring that no caloric restriction was imposed (Fig. 1, A and B, and Fig. S1) (*44*). These feeding regimens were maintained for the duration of the study. Any food hoarded within the cage was removed and excluded from Fig. 1B and Figs. S2-3 as described in the methods.

Food Intake

Measurements of daily food intake throughout each mouse's lifespan showed that feeding increased over time in both sexes, then declined near the end of life in males, similar to previous mouse studies (Fig. 1, A and B, and Fig. S2-3) (*10, 44*). In line with other rodent longitudinal recordings (*45*), females in our study consumed more food relative to their body weight at older ages than males. We also observed sex-specific responses to TRF where 12h-TRF females consumed the same amount as AL, while 12h-TRF males significantly reduced intake compared to AL by 8-14% from 140-539 days (~5-18 months) (Full details of ANOVA results for all figures can be found in Table S1). In contrast, 8h-TRF self-imposed caloric restriction (CR) for the majority of life in both sexes, with intake in females reduced by 10-22% between 140-728 days (~5-24 months) and males reduced by 9-23% between 140-980 days (~5-33 months) relative to sex- and age-matched AL controls. This 8h-TRF schedule, which narrows the daily eating window without explicitly limiting calorie intake as seen in prior mouse and human studies (*46, 47*), presents an alternative strategy for achieving long-term CR in both sexes.

Although actograms (Fig. 1A) show occasional pellet-taking events outside the defined TRF windows, these largely reflect a technical limitation of the feeding system: pellets dispensed at the very end of the dark phase cannot be retracted, allowing a single pellet to remain available and be retrieved during the light period. Importantly, this represents at most one 300 mg pellet per day, accounting for ≤10% of daily intake in 8h-TRF females (lifetime intake 3.0–5.7 g), ≤8% in 12h-

102 TRF females (3.6–5.9 g), ≤9% in 8h-TRF males (3.2–4.7 g), and ≤8% in 12h-TRF males (3.6–5.4
103 g). We quantitatively assessed this behavior across the full lifespan and found the true average
104 proportion of pellets taken outside the feeding window was low, ranging from 5.17–6.34% across
105 feeding groups and sexes (Fig. S1B). In addition, food hoarded within the cage accounted for no
106 more than ~10–12% of the amount removed from the feeder (Fig. S1C). Together, these data
107 suggest that the majority of food intake in both TRF schedules occurs within the intended feeding
108 window. In contrast, some daytime pellet-taking in AL mice is expected, as C57BL/6J mice
109 naturally consume a portion of their food during the inactive phase, with ~75% of intake occurring
110 at night under AL conditions (*9, 10*).

111 **Wheel-Running**

112 Analysis of daily wheel-running recordings for each mouse revealed that individuals in all feeding
113 groups, of both sexes, consistently displayed nocturnal activity, which subsequently declined with
114 age, as anticipated (Fig. 1, A and C, and Figs. S4-5) (*48, 49*). Only 8h-TRF males had increased
115 levels of wheel activity from 224-833 days of age (~7-28 months) with the enhanced activity
116 ranging +36-82% from 329-833 days (~11-28 months) relative to AL. This male-specific
117 difference further underscores the sex-specific effects of TRF on behavior. Additionally, in line
118 with previous work (*10, 50*), the sustained increases in activity under 8h-TRF suggest a healthspan-
119 enhancing effect in male mice.

120

121 TRF Improves the Amplitude of Daily Rhythmic Behaviors

122 We next examined age-related changes in the diurnal profiles of feeding and wheel-running, two
123 well-established rhythmic behaviors, as high-amplitude behavioral rhythms are closely associated

with improved health outcomes (Fig. 2, A and B) (*19, 20, 51, 52*). As intended, TRF reduced the feeding window, shown by longitudinal measurements of the time required for each group to retrieve 90% of their daily food intake from the feeder. Across both sexes, mice under 12h-TRF took 90% of their food within 12h, whereas those under 8h-TRF did so within 8h (Fig. 2C). The time required to reach this threshold declined with age across groups, particularly in females, indicating that feeding became more consolidated in older animals (Fig. 2, A and C). Consistent with this pattern, both TRF groups showed significantly longer daily maximum fasting durations than AL controls, exceeding 10h in the 12h-TRF group and 14h in the 8h-TRF group across both sexes (Fig. 2D).

A Fast Fourier Transform (FFT) analysis of diurnal amplitude, reflecting the strength of daily rhythms, confirmed that TRF increased feeding amplitude and led to a preservation of enhanced rhythmicity with age, particularly in the 8h-TRF group. (Fig. 2, A and E). While the diurnal amplitude of wheel-running declined with age across all groups, 8h-TRF males maintained stronger rhythms throughout life compared to controls (Fig. 2, B and F). In females, TRF modestly increased wheel-running amplitude, with intermittent enhancements relative to controls from ~249 days onward and a sustained elevation in the 8h-TRF group between 543–669 days of age. As mice age, TRF, particularly an 8h window, counteracted the natural decline in behavioral rhythmicity by consolidating food intake and preserving higher-amplitude wheel running activity compared with AL controls.

TRF Improves Body Composition with Limited Effects on Systemic Metabolic Markers

TRF improves body weight and composition

147 Body weights were recorded every 21 days (Fig. 3A, and Fig. S6), and body composition was
148 analyzed every 6 months using nuclear magnetic resonance imaging (EchoMRI, Houston, TX)
149 (Fig. 3, B and C). In females, 12h-TRF without CR lessened age-related gains in body weight by
150 5-8% from 350-686 days of age (~12-23 months) compared with AL controls. This feeding
151 restriction also improved fat vs lean body composition, reducing fat mass while increasing lean
152 mass by 3-4% at 12 and 18 months of age. Unexpectedly, 8h-TRF females with self-imposed CR
153 did not exhibit any further improvements beyond 12h-TRF, in weight or fat/lean composition. In
154 males, 12h-TRF reduced body weight gain by 5-7% from 224-476 days (~7-16 months) and
155 improved fat vs lean composition by 3% at 12 months. 8h-TRF in males enhanced these benefits,
156 lowering body weight gain by 5-16% from 161-749 days (~5-25 months) and improving fat vs
157 lean composition by 3-7% from 6-12 months. Ultimately, these results demonstrate that while 12h-
158 TRF is sufficient to attenuate weight gain and optimize body composition in both sexes, the
159 benefits are more prolonged in females; conversely, males derive significantly greater long-term
160 physiological advantages from a more restrictive 8h-TRF schedule combined with self-imposed
161 CR.

162 **TRF reshapes diurnal RER and EE rhythms**

163 Metabolic changes under TRF were assessed using indirect calorimetry at 19 months of age. Mice
164 were randomly selected and individually housed in Promethion metabolic cages equipped with
165 automated feeders for 5-6 days at room temperature (25°C), followed by 5 days at thermoneutrality
166 (30°C), to assess metabolic parameters independent of the energetic demands of thermoregulation
167 (Fig. S7-8). As expected, 24h respiratory exchange ratio (RER) profiles were significantly
168 influenced by time of day, reflecting normal circadian variation in substrate utilization, and were
169 significantly impacted by the interaction of TRF x time of day (Fig S7A). While TRF did not have

170 a significant main effect on mean 24h RER, post-hoc analyses revealed significantly lower RER
171 values during the delayed onset of feeding in the 8h-TRF group compared with AL controls in
172 both sexes, consistent with extended lipid oxidation during the prolonged fasting period.
173 Additionally, in males housed at room temperature, post-hoc analyses identified higher nocturnal
174 RER values at discrete time points under 8h-TRF, suggesting a shift toward increased carbohydrate
175 utilization during the night and an enhanced diurnal amplitude of RER.
176 24h energy expenditure (EE) profiles also exhibited expected diurnal variation and were
177 significantly influenced by TRF in females, with 8h-TRF trending lower during the daytime/rest
178 phase (Fig. S7B). Post-hoc analyses further revealed that in 8h-TRF females housed at
179 thermoneutrality, daytime EE was significantly reduced at several time points, whereas in males,
180 the minimal impact of TRF was largely restricted to light/dark transitions and feeding/fasting
181 periods across both temperature conditions. These results indicate that TRF modulates EE in a
182 time-dependent manner, with effects shaped by sex and ambient temperature. Impacts on EE were
183 further analyzed by ANCOVA to account for body composition (Fig. S8). Homogeneity of
184 regression slopes was confirmed, and while lean mass significantly influenced outcomes in males,
185 TRF effects on EE remained largely time-specific rather than altering overall 24h EE in either sex.
186 **Glucose homeostasis is moderately improved by 8h-TRF in males**
187 We measured 12h fasting glucose levels and performed glucose tolerance tests at 6, 12, and 18
188 months of age at ZT10 to assess glucose homeostasis. Despite being under circadian control and
189 strongly influenced by feeding (*53*), neither 12h-TRF nor 8h-TRF produced consistent reductions
190 in fasting glucose across all ages as seen in our previous study (Fig. S9A) (*9*). Interestingly, 8h-
191 TRF females exhibited lower fasting glucose at 12 months, but at 18 months levels were
192 significantly higher. In mice, unlike humans, fasting glucose typically declines with age, so the

193 higher levels observed at 18 months in 8h-TRF females may in fact reflect a healthier glucose state
194 (*54*). Glucose tolerance tests also revealed sex-specific effects of TRF. 8h-TRF females showed a
195 modest improvement in glucose homeostasis at 12 months of age, but no impacts were found at 6
196 or 18 months of age in either TRF regimen (Fig. S9, B and C). Males exhibited significant
197 improvements at 6 months in both 12h and 8h-TRF, with modest benefits still apparent at 12
198 months in the 8h-TRF group. Fasting insulin levels from plasma were not significantly altered by
199 either TRF regimen at any age examined (Fig. S10).

200 **Little to no impact on circulating metabolic and inflammatory markers**

201 To determine whether TRF broadly altered systemic metabolic or inflammatory signaling, we also
202 measured circulating levels of leptin, brain derived neurotrophic factor (BDNF), monocyte c
203 chemoattractant protein-1 (MCP-1), tumor necrosis factor α (TNFα), interleukins (IL)-1β, -6, and
204 -10 from 12h fasted plasma collected at ZT10 at 6, 12 and 18 months of age. Overall, TRF had
205 minimal impact on these adipokines, with no sustained differences observed between feeding
206 groups across ages (Fig. S10). An exception was observed at 6 months of age, where males
207 subjected to 8h-TRF exhibited higher plasma BDNF levels than 12h-TRF, suggesting an increased
208 neuroprotective benefit, along with elevated levels of the inflammation-associated chemokine
209 MCP-1. However, these differences were not maintained with aging. Another exception was found
210 at 18 months of age where 12h-TRF males had higher levels of IL-1β and 8h-TRF females had
211 higher levels of MCP-1 suggesting that TRF may have age- and sex-specific effects on
212 inflammatory markers in older animals.

213

214 TRF Slows Age-Related Increases in Frailty Index Values

215 Frailty, a widely used measure of healthspan in aging mice, integrates 31 physiological and

behavioral parameters into a composite index (*55*). Frailty assessments were conducted every 6 months and revealed that both 12h and 8h-TRF significantly reduced frailty index scores at specific ages compared to AL controls (Fig. 4, A-C, and Figs. S11-12). In females, 12h-TRF significantly reduced frailty index scores at 18 months, with hearing loss and body condition assessments defining the key differences between the two groups. 8h-TRF further extended reductions in frailty index from 12 to 24 months, with specific improvements observed in grimace, piloerection, forelimb grip strength, coat condition, ulcerative dermatitis, and body condition scores. Males showed similar trends: 12h-TRF reduced frailty indices between 12 and 18 months, primarily improving grimace and body condition, while 8h-TRF sustained these benefits through 24 months and improved additional parameters, including hearing, piloerection, menace reflex, fur color loss, and coat condition. These results show that TRF significantly lowers age-related frailty in a dose- and sex-dependent manner, with 8h-TRF providing prolonged benefits and improving the greatest number of health measures.

The Age-Related Onset of Health Reports Reveals Sex-Specific Differences and A Delayed Onset in 8h-TRF Males

As mice developed health issues they were reported to veterinary staff for more frequent monitoring. These reports revealed that TRF did not reduce the relative frequency of commonly reported ailments compared to AL (Fig. 4D). Indeed, 8h-TRF males had significantly more reports of body condition scores declining to 2 (Scored 1-5 with: 1 being emaciated, 2 underconditioned, 3 ideal condition, 4 overconditioned, and 5 obese) (Fisher's exact test 8h-TRF vs AL: Body Condition Score=2, $P < 0.05$). However, we observed a clear sex-dependent pattern in the types

238 and frequencies of reported conditions. Females, regardless of feeding group, were significantly
239 more likely to be reported for ulcerative dermatitis (Fisher's exact test females vs males: $P <$
240 0.0001), rectal prolapse ($P < 0.0001$), and hind limb paralysis (often associated with spinal tumors,
241 $P < 0.001$). In contrast, males were more frequently reported for external tumors and abdominal
242 masses (Fisher's exact test females vs males: $P < 0.0001$), as well as low Body Condition Score=2
243 ($P < 0.0001$). The onset of age-related health issues also differed by sex, with 8h-TRF delaying
244 the median health report onset by 52 days in males only compared to AL controls (Log-rank
245 Mantel-Cox, $P = 0.0018$) (Fig. 4E). Additionally, while there were no significant differences under
246 TRF, overall, females overall spent significantly fewer days on health report prior to death, than
247 males (Fig. 4F). Altogether this demonstrates there is sex-specificity in the development of
248 common husbandry related-disease.

249

250 TRF Has Minimal Impacts on Hematological Markers

251 To determine whether lifelong TRF impacted hematological markers, which are emerging as
252 predictors of systemic health and aging (*56*), we assessed complete blood counts from whole blood
253 at 6, 12 and 18 months of age. Overall, TRF had minimal effects on circulating blood parameters
254 in either sex. Red blood cell counts (RBC), hemoglobin, hematocrit, red cell indices including
255 mean corpuscular volume (MCV), mean corpuscular hemoglobin (MCH), and mean corpuscular
256 hemoglobin concentration (MCHC), and platelet counts were largely unchanged across feeding
257 regimens (Figs. S13-14). TRF also had no significant impacts on total white blood cell counts or
258 leukocyte subtypes (Fig. S15). The only notable exception was observed in females at 18 months
259 of age, where 8h-TRF mice displayed higher RBC counts accompanied by lower MCV (smaller
260 RBCs; typically indicate older, longer maintained cells) and MCH compared to AL controls (Fig.

261 S13). Given that old age in mice is commonly associated with reduced RBC survival (*57*), this
262 pattern might reflect improved maintenance of RBC homeostasis rather than a pathological shift.
263 Importantly, MCHC, hemoglobin levels, and hematocrit were unchanged in 8h-TRF females,
264 indicating preserved hemoglobin concentration within cells and maintained oxygen-carrying
265 capacity.

266

267 8h-TRF Extends Lifespan in Males Only

268 For the first time, we were able to investigate the impact of circadian aligned TRF with regular
269 chow diet, on lifespan in mice (Fig. 5A, and Tables S2-3). In females, no significant extension of
270 median lifespan was observed with either 12h-TRF or 8h-TRF. Median survival was 715 days and
271 729 days, respectively, compared to 694 days in AL controls. In males, 12h-TRF also failed to
272 extend lifespan, with a median survival of 839 days compared to 818 days in AL, a finding now
273 reproduced across two independent experiments (Fig. S16). Interestingly, 8h-TRF with lifelong
274 self-imposed CR, significantly improved overall survival for males (Log-rank Mantel-Cox, P =
275 0.0001). Median lifespan increased by approximately 12%, reaching 916 days, and maximal
276 lifespan was prolonged by ~3% (Fisher's exact test, P = 0.0038). Though TRF is beneficial for
277 improving health in both sexes, its capacity to extend lifespan appears to be feeding window- and
278 sex-dependent.

279

280 Sex-Dependent Differences in Disease Types and Incidence at Death

281 After death, each mouse underwent gross necropsy and histopathological analysis by a veterinary
282 pathologist to determine the types of diseases that contributed to its debilitation (Fig. 5B, and

Tables S4-6). As shown previously (*10*), the types and relative frequency of diseases were similar for males across all feeding conditions with the most common cause of death or debilitation being neoplasia (Fig. 5B, and Table S7). Along with the delayed onset of health reports, overall, this supports that rather than preventing disease, 8h-TRF delays the development of age-related diseases in males.

However, a few specific neoplastic subtypes were differentially affected by TRF. In males, bronchioloalveolar adenomas, benign tumors, were significantly increased in both 12h-TRF and 8h-TRF groups compared to AL controls. (Fisher's exact tests AL vs TRF: 12h and 8h, $P < 0.05$). In females, hepatocellular adenomas, were significantly more frequent in the 8h-TRF group (Fisher's exact tests AL vs TRF: 8h $P < 0.05$). While this indicates increased growth of tumors with malignant potential, the absence of a corresponding increase in carcinomas suggests that TRF may shift the spectrum of pathology toward less aggressive neoplastic lesions rather than completely preventing tumorigenesis.

TRF did not reduce the overall occurrence of disease in females either. However, females developed neoplasms far less frequently than males (Fisher's exact tests females vs males: Adenoma in liver, $P < 0.05$; Carcinoma in liver and lung, each $P < 0.0001$; Histiocytic sarcoma in liver and lung, each $P < 0.0001$; Histiocytic sarcoma in spleen, $P < 0.001$; Acidophilic macrophage pneumonia in lung, $P < 0.0001$; Adenoma in lung, $P < 0.0001$). Instead, most females were debilitated by glomerulonephritis in the kidneys and had a higher incidence of lymphoma than males (Fisher's exact tests females vs males: Lymphoma in liver, kidney, spleen, each $P < 0.05$; Glomerulonephritis, $P < 0.0001$). These results have revealed pronounced differences in neoplasia and development of other age-related morbidities between the sexes.

306 **TRF Extends Healthspan, With More Prolonged Benefits in Females**

307 While TRF improved and attenuated age-related changes in several markers of health, we next
308 aimed to quantify both the magnitude and duration of its overall impact by measuring healthspan.
309 Frailty index is commonly used to determine healthspan (*55, 58*), but it cannot incorporate the
310 impact of behavioral changes in wheel-activity and food consumption and can miss important
311 physiological changes in the time between assessments. To generate a continuous healthspan
312 index, we integrated frailty with 12 additional health measures by first normalizing each data set
313 (mean = 0, standard deviation = 1), then scaling the parameter directionally by providing context
314 based on whether higher or lower values reflected better health (e.g., high wheel-running activity
315 was scaled positively, while low frailty scores were inverted and also scaled positively) (Fig. 6A),
316 and finally summing the values across age points (Fig. 6B). With higher values reflecting better
317 health, we found that both females and males under TRF had significantly improved healthspan
318 indices throughout life compared to AL controls (Fig. 6, B and C). In 12h-TRF females, this
319 improvement in health was maintained from the onset of TRF until 774 days of age (~26 months).
320 In 8h-TRF females, health benefits persisted until 879 days of age (~29 months), and these mice
321 remained healthier than the 12h-TRF group until 858 days (~29 months). In males, 12h-TRF also
322 improved the healthspan index through 879 days of age (~29 months), whereas 8h-TRF extended
323 these improvements to 963 days (~32 months) and were significantly healthier than the 12h-TRF
324 group until 942 days (~31 months). Importantly, these healthspan indices strongly correlate with
325 lifespan in both sexes, demonstrating that this integrated metric captures biologically meaningful
326 health outcomes (Fig. 6D).

327 We also found that health declines were more delayed in females than in males, particularly under
328 TRF. Using subjective thresholds of '0' or '-5' (black dashed lines), AL females crossed the '-5'

329 threshold more than 100 days later than AL males, indicating that females maintain better health
330 for longer, especially relative to their total lifespan. Under 12h-TRF, females not only had
331 prolonged healthspan relative to controls at these thresholds, but also crossed the '0' threshold
332 more than 200 days later than males on the same TRF regimen. While 8h-TRF extended health
333 above the '0' threshold by approximately 500 days relative to AL in both sexes, this also made up
334 a greater portion of the females lifespan. Together, these results demonstrate that TRF extends
335 healthspan in both sexes and further suggest that, despite the absence of lifespan extension in
336 females, females in both TRF regimens remain healthier for a greater proportion of their lifespan
337 than males.
338 To validate our findings of TRF-induced healthspan extension further, we also applied a previously
339 published summary metric, Frailty-Adjusted Mouse Years (FAMY) (*59*). FAMY, which relies
340 solely on frailty scores, similarly detected a significant healthspan increase in 8h-TRF males (Fig.
341 S17A). The lower frequency of frailty assessments in our study, performed only once every six
342 months, likely contributes to the banded distribution of FAMY scores and may explain
343 discrepancies between the two methods. Nevertheless, FAMY showed strong correlations with
344 lifespan across all groups (Fig. S17B). These results support the robustness of our healthspan
345 measurements and suggest that our more comprehensive, higher-resolution index may be better
346 suited for detecting healthspan changes in females.
347

348 **Discussion:**

349 Previous studies have established that TRF improves circadian rhythms, ameliorates metabolic
350 syndrome, and improves overall health in obesity models consuming a 'Western diet' high in fats
351 and sugars (*28-32*). We expand on these findings by revealing that circadian aligned TRF confers

352 significant, long-term health benefits even under normal nutritional conditions. We show that,
353 depending on the feeding window and sex, TRF prolonged higher amplitudes of daily rhythms in
354 feeding and wheel-running, which are known to feed back on the circadian clock to drive robust
355 molecular and behavioral oscillations (*14, 15, 17, 47, 60-62*). Both TRF paradigms were sufficient
356 to significantly reduce age-related increases in weight and fat mass, having the largest impact
357 during midlife. TRF similarly slowed the age-related decline in lean composition, which may also
358 contribute to the observed improvements in adiposity and suggests that TRF can delay the onset
359 of functional disabilities (*63-65*). We also present novel findings that both TRF windows reduce
360 frailty index in females and males, as in CR and intermittent fasting studies (*66-70*). Veterinary
361 health reports were largely sex-dependent, and overall TRF did not alter the types of deficits
362 observed. Notably, 8h-TRF males displayed a higher proportion of low body condition scores
363 (score of 2), but this occurred alongside a delayed onset of health issues and overall increased
364 lifespan and likely reflects the survival of more mice to advanced ages rather than a detrimental
365 effect of TRF. Consistently, no differences in body condition score were observed at 30 months in
366 males within the individual frailty assessments. Altogether, this demonstrates that TRF does not
367 merely act as a remedial strategy to 'rescue' poor health but can actively improve behavioral and
368 physiological markers of health for both sexes under normal metabolic aging conditions.

369 Despite these robust improvements in health, TRF-induced reductions in body weight and
370 adiposity were not accompanied by consistent improvements in glucose tolerance or sustained
371 alterations in fasting glucose, insulin, leptin, or circulating inflammatory markers. These findings
372 indicate that the metabolic benefits of TRF do not require large shifts in systemic endocrine or
373 inflammatory signaling. Instead, they suggest that TRF may promote health through alternative
374 mechanisms, such as enhanced circadian organization, behavioral rhythmicity, or tissue-specific

375 metabolic adaptations. Consistent with this, 24h EE and RER profiles revealed that TRF primarily
376 reshaped temporal patterns of substrate utilization and EE, rather than altering overall 24h mean
377 values. Importantly, these benefits occurred without detrimental effects on hematological health.
378 TRF had no impact on red blood cell indices, platelet counts, or immune cell abundance across
379 aging, and the modest changes observed in 8h-TRF females were not associated with impaired
380 oxygen-carrying capacity, supporting the long-term physiological safety of circadian aligned TRF.

381 By integrating measures of frailty, physiology, and behavior into a novel, comprehensive
382 healthspan index, we demonstrate that TRF significantly enhances healthspan in both sexes, with
383 proportionally greater benefits in females relative to their lifespan. We also found that 12h-TRF
384 strongly delayed the initial healthspan decline in females during middle-age, whereas its effect in
385 males at the same threshold is minimal. However, this approach may oversimplify sex-specific
386 differences, as males and females exhibit distinct patterns of health deficits that associate
387 differently with longevity. A single healthspan scale as used here might not adequately reflect
388 these complex, sex-dependent impacts on aging. Although females generally show better health
389 indices, we found they had shorter lifespans than males, highlighting a potential disconnect
390 between this healthspan index and ultimate survival outcomes. It is also important to note, that sex
391 differences observed in mice may not fully translate to humans, as differences in circadian
392 rhythms, hormonal cycles and reproduction, and metabolic rate can alter the magnitude and timing
393 of sex-specific responses to TRF (*71-74*). Regardless, this sex-specific response in healthspan
394 likely reflects a combination of biological factors. Estrogen is known to confer broad protective
395 effects on health and aging (*75*), which may explain the overall female advantage even under AL
396 feeding, and is known to feedback onto the circadian clock (*76-78*). With recent literature showing
397 that females possess a more robust circadian system (*71*), this may underlie their enhanced

398 responsiveness to circadian-based interventions. Recent studies have found that females express a
399 greater number of rhythmic genes, display higher amplitude rhythms, and are more sensitive to
400 external cues (*79-81*). As such, TRF may more effectively enhance rhythms at the molecular level
401 to promote health in females (*19, 20*).

402 For the first time, we show that aligning feeding to the active phase under 12h-TRF does not extend
403 lifespan. However, a narrower feeding window of 8h-TRF along with self-imposed CR conferred
404 strong lifespan extension in males. These results contrast with previous studies showing that
405 lifelong 20% CR, adjusted relative to age-related changes in AL feeding, extends lifespan by
406 40.6% in female and 24.4% in male C57BL/6J mice (*82*). While our 8h-TRF mice maintained
407 ~20% CR for nearly half of their lifespan, both males and females gradually lessened the degree
408 of CR relative to AL feeding shortly before reaching median lifespan. Despite this, 8h-TRF males
409 gained a 12% extension in median lifespan, indicating that even a lower degree of CR is still
410 impactful in males. In contrast, females appear to require a sustained degree of CR ≥20% to see
411 any lifespan benefits. Alternatively, the duration of fasting may be more crucial for female
412 lifespan, as longer fasting periods with CR have enhanced lifespan effects in females (*8, 82*), but
413 not in males (*10*). The mechanisms underlying these sex-dependent differences in response to CR
414 and TRF are not fully understood, especially between different strains of mice (*5, 82*), but are
415 likely influenced by a complex interplay of factors such as differences in nutrient sensing and
416 metabolic pathways, DNA repair, and the effects of sex hormones (*41, 71, 83*).

417 Survival curves for AL mice unexpectedly showed an 18% increase in median survival for males
418 compared to females, contrary to the common trend in mammalian studies where females typically
419 live longer due to the genetic advantage of a backup X chromosome and the protective effects of
420 estrogen (*84, 85*). However, in C57BL/6J mice, lifespan outcomes are inconsistent possibly due to

421 genetic drift within the isogenic line as well as environmental variations between experiments (*85-*
422 *88*). While genetic factors may play a role, the shorter lifespan in females could stem from
423 enhanced cold sensitivity and higher thermoregulatory energy demands (*89-92*). The smaller
424 bodied females, needing more energy to maintain body temperature as evidenced by the
425 pronounced increase in food intake with age, may have been adversely affected by the harsher
426 individual housing conditions without nesting material. Although lower body temperatures can
427 extend lifespan (*93, 94*), cold stress can also divert energy away from and impair metabolic,
428 immune, and reproductive functions (*95, 96*). Future studies will be needed to directly evaluate
429 thermogenic pathways underlying these sex-specific effects, including gene expression in brown
430 adipose tissue (*47*). In addition, evaluating TRF and lifespan outcomes under thermoneutral
431 housing conditions or with access to nesting material will help disentangle the relative roles of
432 thermoregulation and feeding timing in shaping healthspan and longevity.

433 Health report monitoring and post-death histopathological analyses revealed significant
434 differences between the sexes in the progression of age-related diseases, particularly in neoplasia.
435 With the exception of lymphoma, female mice had significantly lower occurrences of neoplasms
436 in the liver, lung, kidney, and spleen which supports a growing body of data that females have
437 greater resistance to cancer (*97-99*). This resistance is largely attributed to sex differences in
438 immunity, mutational burden, and DNA repair, as well as the protective role of X-linked tumor
439 suppressor genes and their interaction with the p53 pathway in females. Although mechanistic
440 experiments are beyond the scope of this study, RNA-sequencing and proteomic analysis of the
441 liver, the tissue most affected by neoplasia in males and least in females, could help to dissect the
442 molecular mechanisms underlying these sex-specific differences in cancer development under
443 TRF. These mechanisms are likely to include pathways regulating the cell cycle and cellular

444 proliferation. Females in this cohort were instead most susceptible to kidney failure due to
445 glomerulonephritis, similar to a previous study (*100*). This condition has been linked to menopause
446 in women, with its progression often accelerating after the decline in estrogen levels (*101*). In
447 mice, this disease can be further exacerbated in the absence of the *estrogen receptor alpha* gene
448 (*102*), emphasizing the protective role of estrogen signaling and uncovering renal disease as a
449 potential biomarker of reproductive aging.

450 One limitation of this study was the inability of the automated feeders to retract or block a food
451 pellet that goes uneaten beyond the restricted food intake window. This meant that often, a single
452 pellet could be taken by the mouse, outside of its 12h or 8h-TRF window. Additionally, some mice
453 had the tendency to hoard pellets within their cage, leading again to food availability outside of
454 the TRF window, a trait that has already been shown in aged mouse populations (*44*). However, a
455 single daytime pellet accounted for ≤6.34% of total caloric intake, and after subtracting hoarded
456 food, mice consumed ≥90% of the pellets taken from the feeder during the correct feeding
457 windows. These findings, along with evidence that TRF 5 out of 7 days per week regimens still
458 improves metabolic health in mice (*39*), and lifespan in flies (*103*), suggest that moderate TRE
459 adherence may still prolong healthspan and be compatible with modern human lifestyles.

460 Our study focused on TRF regimens initiated in early adulthood and maintained throughout life,
461 leaving the efficacy of late-life implementation yet to be determined. Short-term studies indicate
462 that TRF in the elderly can reduce high-fat diet-induced inflammation and metabolic dysfunction,
463 and studies with CR in aged mice still provided health and lifespan benefits (*104-106*). However,
464 these benefits provide diminishing returns, dependent on the age at which an intervention is started.
465 Furthermore, as most of the observed benefits occurred through mid-life and the onset of old age,
466 this raises the question of whether a lifelong intervention is necessary, or if stopping TRF before

467 old age might be sufficient, or even preferable, to avoid potential late-life trade-offs. This
468 possibility is supported by other models, where short-term TRF applied in flies earlier in life
469 increases longevity and functional health even after returning to AL feeding (*42, 103, 107*), and
470 by some evidence that TRF in aged mice had negative impacts on lean mass and cardiovascular
471 health (*108*).

472 Beyond the life stage at which TRF is initiated, the specific timing of the feeding window relative
473 to the internal circadian clock represents a critical variable in metabolic optimization. In this study,
474 the 8h-TRF window was intentionally positioned in the middle of the active period (ZT14–ZT22),
475 instead of the onset (ZT12), as this is consistent with several previous mouse studies (*29, 109*),
476 and prior work in humans suggests that delaying breakfast and/or advancing the final meal can
477 confer metabolic benefits (*110*). Thus, it remains possible that the enhanced healthspan and
478 lifespan benefits observed with 8h-TRF reflect not only feeding duration, but also a shift in the
479 midpoint of daily caloric intake, an aspect of circadian alignment that warrants further
480 investigation. While we observed robust benefits of 8h-TRF in mice, it is also important to note
481 that direct translation to humans is limited by differences in metabolic rate and circadian timing
482 (*73*). In practice, fasting intervals in mice correspond to approximately ~2.7–3.6 times longer
483 relative windows in humans, so caution is warranted when extrapolating the duration and timing
484 of TRF across species (*73, 74*).

485 The absence of direct cardiovascular assessments remains a limitation, particularly as
486 cardiovascular disease is a prevalent age-associated pathology in mice. Given the limited data from
487 long-term studies directly evaluating cardiovascular effects of TRF/TRE (*111-113*), future studies
488 incorporating dedicated measures of cardiac function, structure, and blood pressure will be

489 essential to determine how timed feeding influences cardiovascular health across the lifespan,
490 particularly under conditions of normal metabolic aging.

491 In conclusion, our study provides compelling evidence that the early initiation of circadian aligned
492 TRF either via a 12h or 8h window significantly improves healthspan in both sexes, more so in
493 females proportional to lifespan, and that 8h-TRF robustly extends lifespan in males. While this
494 still warrants further exploration in additional mouse strains and at varying ages of onset, taken
495 together this highlights the potential of TRF as a practical, non-pharmacological intervention to
496 prolong the health quality of human lifespans.

497 **Figures and Legends:**

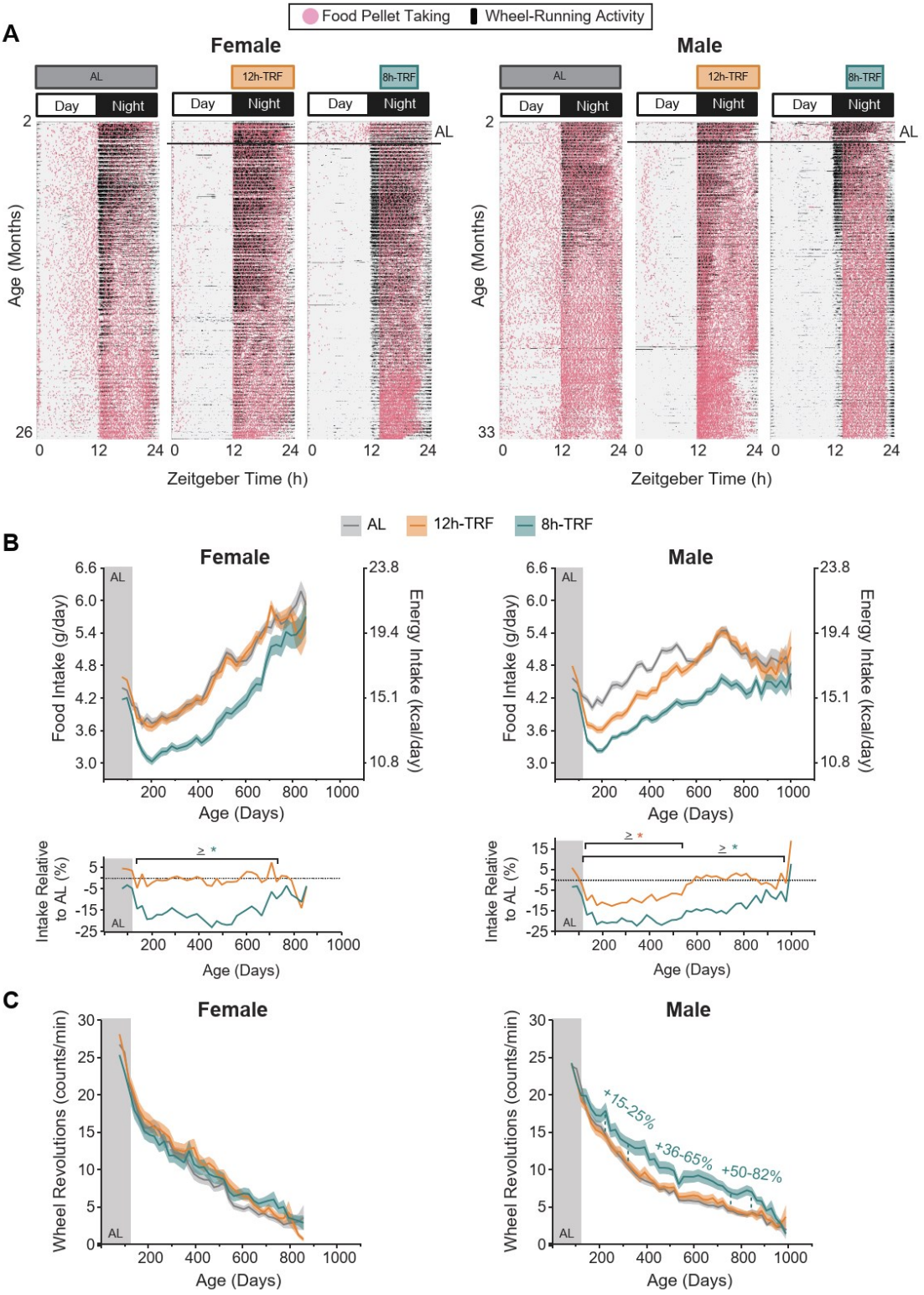

498 **Figure 1: Circadian aligned TRF reduces feeding and improves wheel-running activity in a**
499 **feeding window- and sex-dependent manner.** (**A**) In females 2-26 months of age and males 2-
500 33 months of age, representative actograms of individual mice show wheel-running (black mark)
501 and food pellet taking (pink dot) activity over the course of the 24-hour (h) light:dark cycle. Black
502 horizontal line shows ends of *ad libitum* (AL) baseline feeding for the TRF groups at 4 months of
503 age. (**B**) (*Top*) Longitudinal profiles of average daily food intake and energy intake with age and
504 (*Bottom*) percent differences in CR relative to AL controls with age. Two-way ANOVA: Females:
505 Age=****, Feeding=****, Interaction=****; Males: Age=****, Feeding=****, Interaction=****
506 (Full details of ANOVA results for each figure can be found in Table S1). (**C**) Longitudinal profiles
507 of average daily wheel revolutions with age. Two-way ANOVA: Females: Age=****,
508 Feeding=**, Interaction=ns; Males: Age=****, Feeding=****, Interaction=ns. <u>B and C:</u> AL
509 baseline feeding (Gray area). TRF feeding conditions (White area). Each point represents mean of
510 21 days ± SEM (shaded regions). Asterisks/percents represent significant differences in TRF vs
511 AL (*P ≤ 0.05; **P ≤ 0.01; ***P ≤ 0.001; ****P ≤0.0001) as determined by two-way ANOVA
512 and Tukey's post-hoc. Females N=71-103 per group. Males N=71-97 per group.

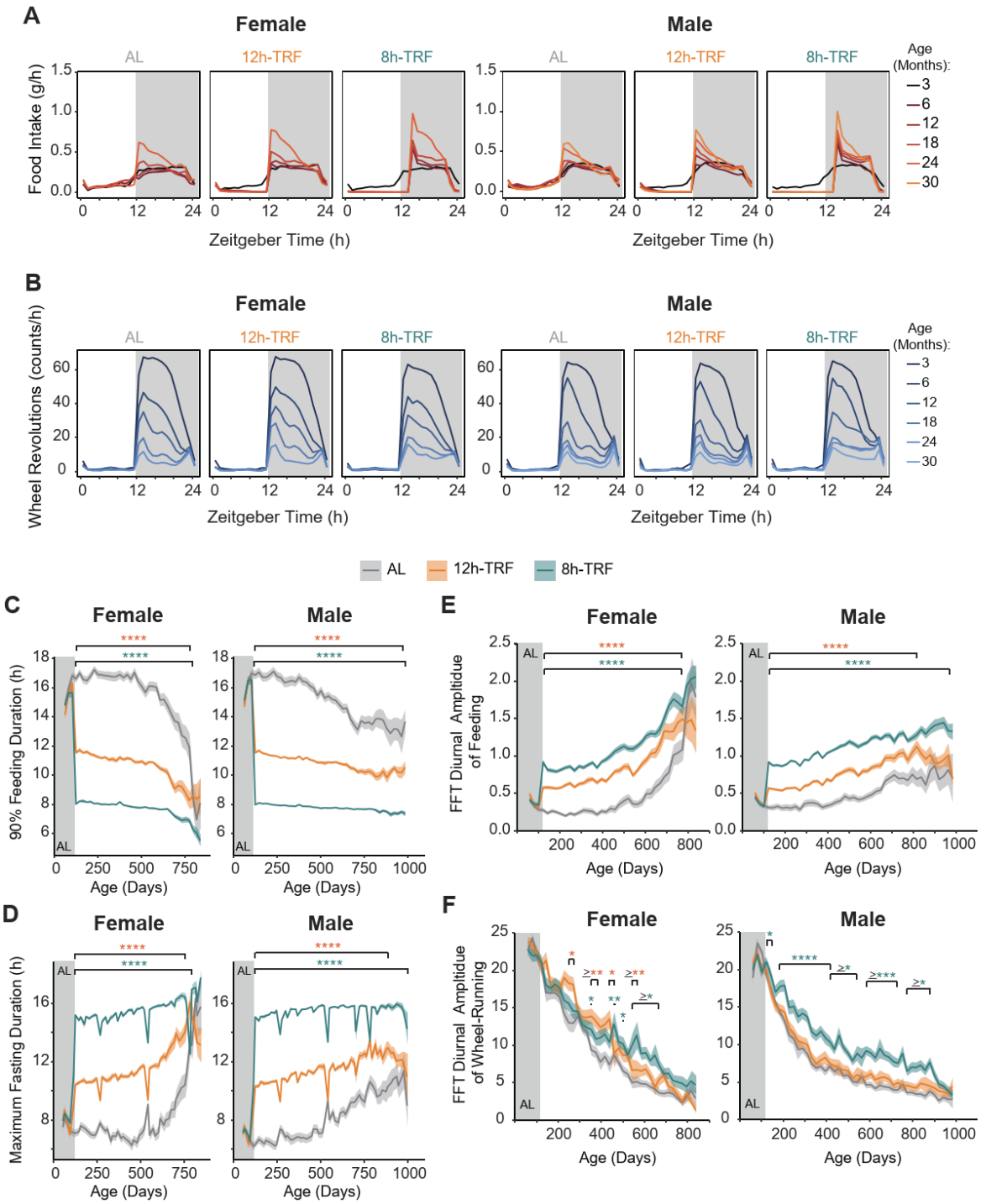

513 **Figure 2: TRF improves the amplitude of daily feeding and wheel-running rhythms.** (**A**) 24h
514 profiles of feeding and (**B**) wheel-running starting at 3 and then every 6 months of age. 12h light
515 (white area), 12h dark (gray area). (**C**) Longitudinal plots for daily time it takes each group of mice
516 to take 90% of their daily intake from the feeder. Type III ANOVA (Wald χ^2): Females: Age=****,

517 Feeding=****, Interaction=****; Males: Age=****, Feeding=****, Interaction=****. (**D**)
518 Longitudinal plots for daily maximum fasting times achieved. Type III ANOVA (Wald χ^2):
519 Females: Age=****, Feeding=****, Interaction=****; Males: Age=****, Feeding=****,
520 Interaction=****. To note: Large, transient dips in fasting due to interruptions in data acquisition
521 (e.g., fasting blood collection attempt and computer outage). (**E**) Longitudinal FFT plots of the
522 diurnal amplitude of feeding with age. Type III ANOVA (Wald χ^2): Females: Age=****,
523 Feeding=****, Interaction=****; Males: Age=****, Feeding=****, Interaction=****. (**F**)
524 Longitudinal FFT plots of the diurnal amplitude of wheel-running with age. Type III ANOVA
525 (Wald χ^2): Females: Age=****, Feeding=*, Interaction=****; Males: Age=****, Feeding=****,
526 Interaction=***. C-F: AL baseline feeding (Gray area). TRF feeding conditions (White area). Each
527 point represents mean of 14 days ± SEM (shaded regions). Asterisks represent significant
528 differences in TRF vs AL (*$P \leq 0.05$; **$P \leq 0.01$; ***$P \leq 0.001$; ****$P \leq 0.0001$) as determined
529 by type III ANOVA (Wald χ^2) and Holm's post-hoc. For all panels: Females N=71-103 per group.
530 Males N=71-97 per group.

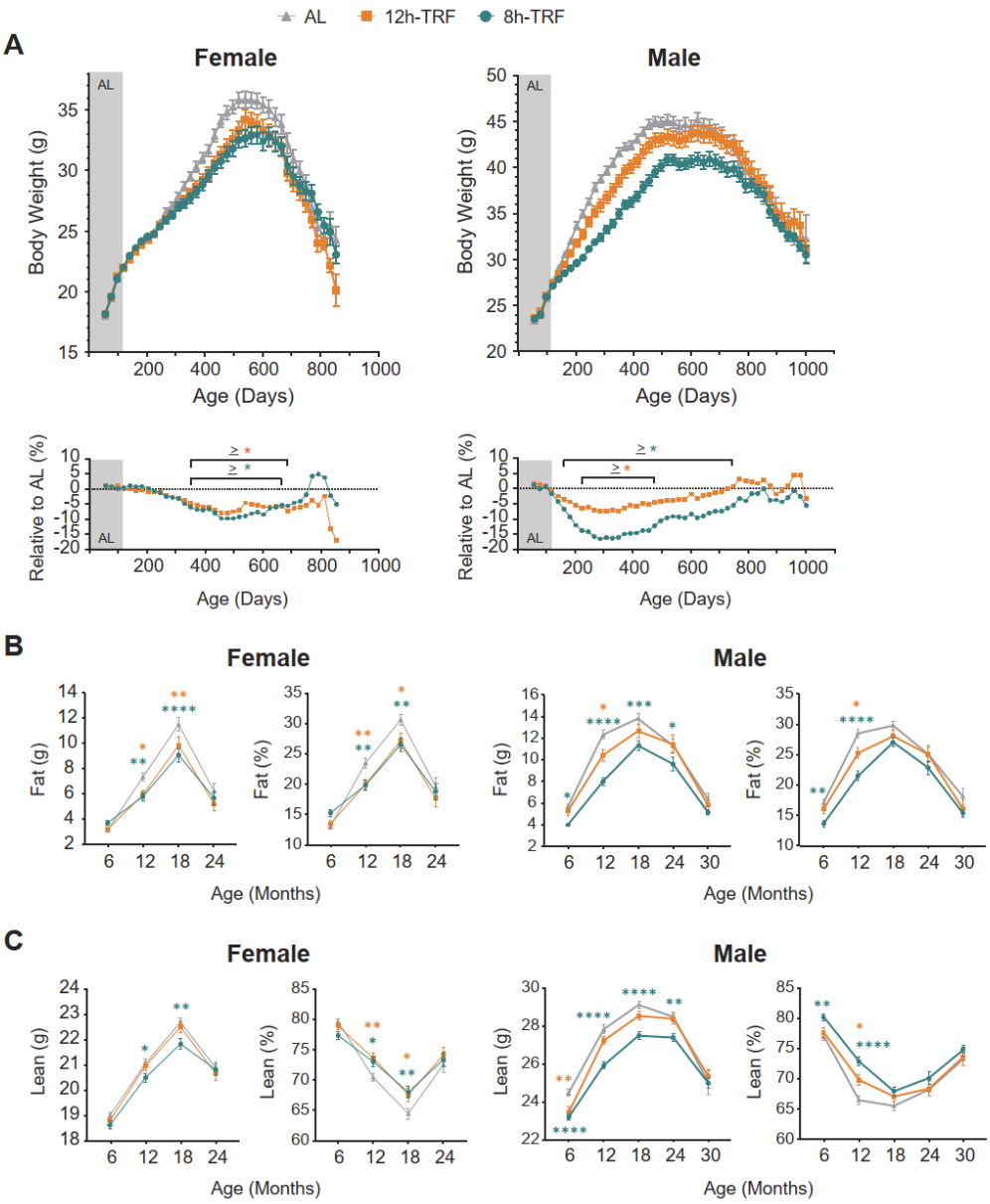

Figure 3: A 12h TRF window is sufficient to reduce body weight and fat mass in both sexes. (**A**) (*Top*) Longitudinal profiles of body weight and (*Bottom*) percent differences in body weight relative to AL controls with age. Two-way ANOVA: Females: Age=****, Feeding=****, Interaction=****; Males: Age=****, Feeding=****, Interaction=****. AL baseline feeding (Gray area). TRF feeding conditions (White area). Each point represents mean of 21 days (cage change) ± SEM (bars). Asterisks represent significant differences in TRF vs AL (*P ≤ 0.05; **P ≤ 0.01; ***P ≤ 0.001; ****P ≤0.0001) as determined by two-way ANOVA and Tukey's post-hoc. Females

538 N=76-103 per group. Males N=76-102 per group. (**B**) Total fat mass as a percentage of body
539 weight with age. (**C**) Total lean mass as a percentage of body weight with age. B and C: Means
540 every 6 months ± SEM (bars). Asterisks represent significant differences in TRF vs AL as
541 determined by two-way ANOVA and Tukey's post-hoc. Females 6-24 months: AL, N=43-101.
542 12h-TRF, N=32-71. 8h-TRF, N=38-72. Males 6-30 months: AL, N=23-102. 12h-TRF, N=19-77.
543 8h-TRF, N=36-75.

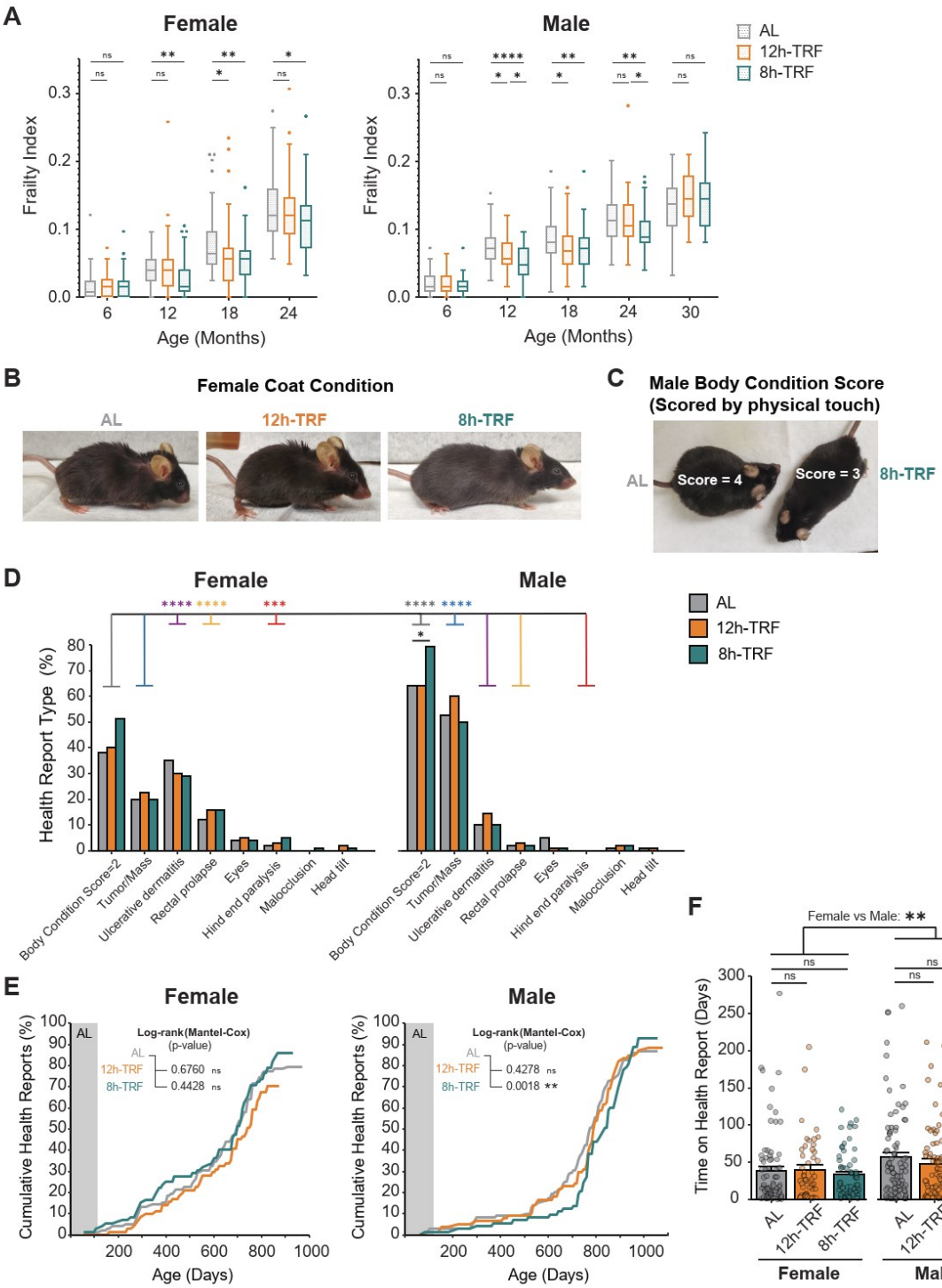

Figure 4: TRF reduces frailty index in both sexes but only delays onset of health reports in males. (**A**) Boxplots of frailty index scores every 6 months. Two-way ANOVA: Females: Age=****, Feeding=****, Interaction=ns; Males: Age=****, Feeding=****, Interaction=**.

Asterisks represent significant differences in TRF vs AL (*P ≤ 0.05; **P ≤ 0.01; ***P ≤ 0.001; ****P ≤0.0001) as determined by two-way ANOVA and Tukey's post-hoc. Females: AL, N=44-79. 12h-TRF, N=34-74. 8h-TRF, N=40-74. Males: AL, N=23-79. 12h-TRF, N=22-78. 8h-TRF, N=39-76. (**B**) One example parameter contributing to reduced frailty index in 8h-TRF females: coat condition, P < 0.05 at 24 months compared to AL. (Full list see Fig. S11). (**C**) One example parameter contributing to reduced frailty index in 8h-TRF males: body condition score, P < 0.05 12-18 months compared to AL. (Full list see Fig. S12). (**D**) Percentage of mice in each feeding group and sex reported to veterinary staff for Body Condition Score=2, Tumor/Mass, Ulcerative dermatitis, Rectal prolapses, Eye ulcerations/swelling, Hind end paralysis, Malocclusions, and Head tilts. Black asterisks represent significant differences in TRF vs AL, and all other colors represent male vs female comparisons as determined by contingency tables and Fisher's exact tests. (**E**) Cumulative curve showing the percentage of veterinary health reports filed in each group with age. Log-Rank Mantel-Cox Test. (**F**) Time spent on health report until death. Two-way ANOVA: Sex=**, Feeding=ns, Interaction=ns. Data shown as mean ± SEM.

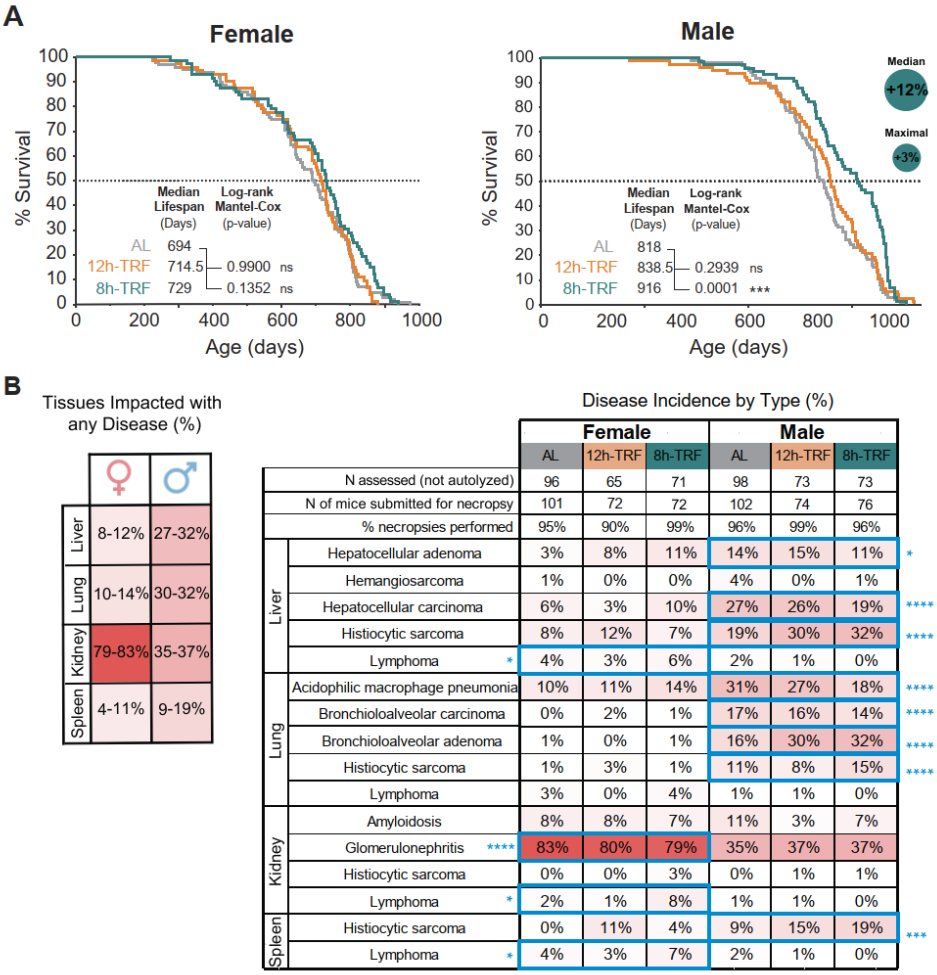

Figure 5: 8h-TRF extends lifespan in males. (**A**) Kaplan-Meier survival curves and day median lifespan reached. Log-Rank Mantel-Cox Test for significant difference in overall survival TRF vs AL. Fisher's exact test for maximal survival TRF vs AL. Females N=72-99 per group. Males N=73-99 per group. (**B**) (*Left*) Histopathology results showing the percentage incidence of any disease type in the most impacted tissue types between females and males and (*Right*) incidence by specific disease type within these tissues separated by sex and feeding group (Full table with all tissues and diseases shown in Tables S4-6). Significant differences in females vs males highlighted by blue boxes and shown with blue asterisks (*P ≤ 0.05; **P ≤ 0.01; ***P ≤ 0.001; ****P ≤0.0001) as determined by contingency tables and Fisher's exact tests.

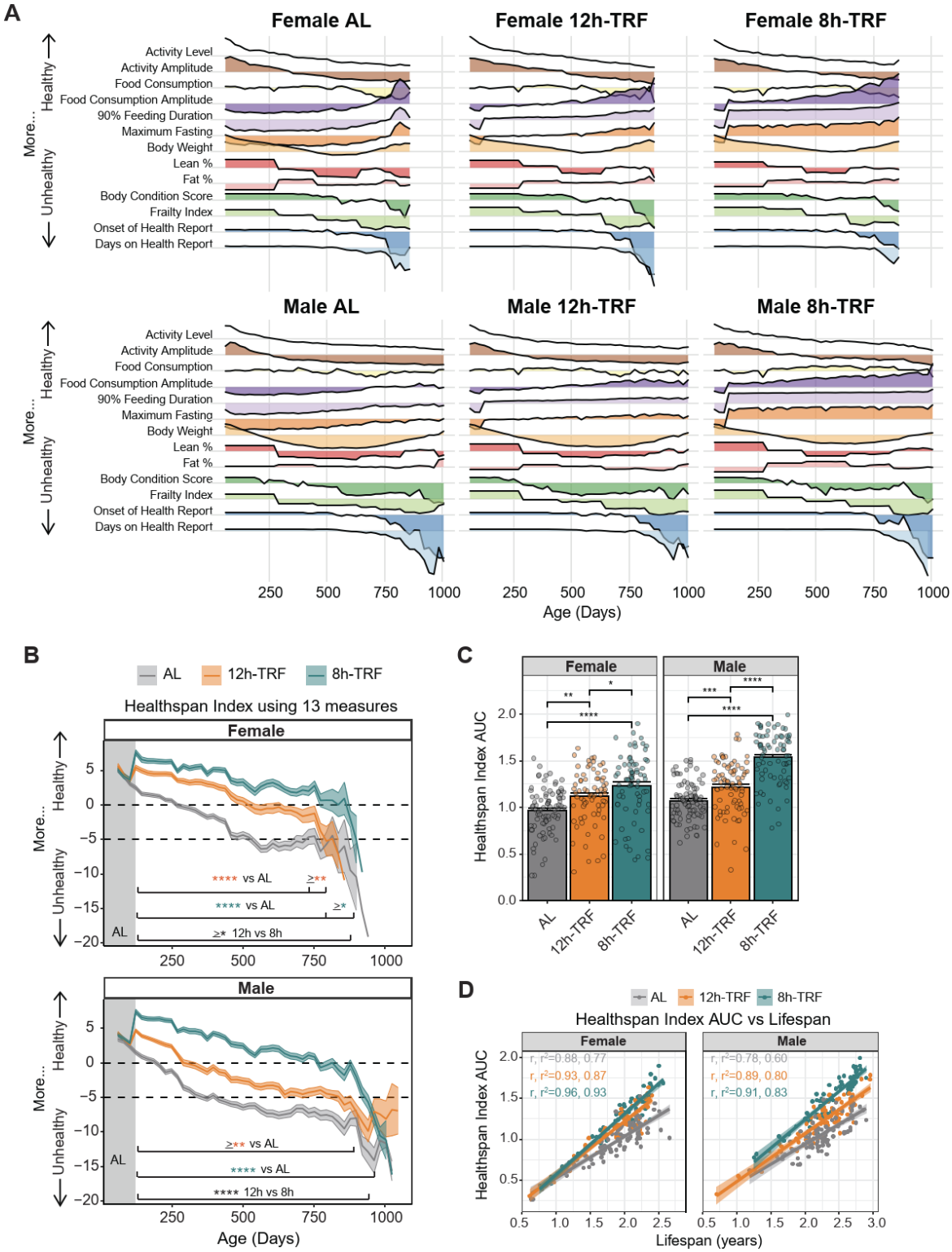

Figure 6: TRF improves healthspan in both sexes. (**A**) Ridgeline plots for each of the 13 health measures recorded throughout the experiment. All parameters were standardized (mean = 0, SD =

572 1) and, where appropriate, oriented in the positive direction to reflect better health. (**B**) Healthspan
573 index summing the 13 health measures for each group from panel A. Higher values indicate better
574 health and lower values poorer health. Dashed lines (black) mark the age at which each group's
575 index crosses subjective thresholds of 0 and –5. Type III ANOVA (Wald χ^2): Females: Age=****,
576 Feeding=****, Interaction=****; Males: Age=****, Feeding=****, Interaction=ns. Each point
577 represents mean of 21 days ± SEM (shaded regions). Asterisks/percents represent significant
578 differences (*P ≤ 0.05; **P ≤ 0.01; ***P ≤ 0.001; ****P ≤0.0001) as determined by type III
579 ANOVA and Holm's post-hoc. (**C**) Area under the curve (AUC) for healthspan index in females
580 and males. Type III ANOVA: Sex=****, Feeding=****, Interaction=***. Mean ± SEM (bars).
581 Asterisks represent significant differences as determined by type III ANOVA and Holm's post-
582 hoc. (**D**) Correlation plots of healthspan AUC vs lifespan in years. Correlation coefficients (r) and
583 coefficients of determination (r^2) shown.

584 **References and notes:**

585 1. D. Costa, Health and the Economy in the United States, from 1750 to the Present. *J Econ*
586 *Lit* **53**, 503-570 (2015).
587 2. J. W. Vaupel, Biodemography of human ageing. *Nature* **464**, 536-542 (2010).
588 3. C. L. Green, D. W. Lamming, L. Fontana, Molecular mechanisms of dietary restriction
589 promoting health and longevity. *Nat Rev Mol Cell Biol* **23**, 56-73 (2022).
590 4. A. McKay *et al.*, An automated feeding system for the African killifish reveals the impact
591 of diet on lifespan and allows scalable assessment of associative learning. *Elife* **11**, (2022).
592 5. A. Di Francesco *et al.*, Dietary restriction impacts health and lifespan of genetically diverse
593 mice. *Nature* **634**, 684-692 (2024).
594 6. S. J. Mitchell *et al.*, Daily Fasting Improves Health and Survival in Male Mice Independent
595 of Diet Composition and Calories. *Cell Metab* **29**, 221-228 e223 (2019).
596 7. H. H. Pak *et al.*, Fasting drives the metabolic, molecular and geroprotective effects of a
597 calorie-restricted diet in mice. *Nat Metab* **3**, 1327-1341 (2021).
598 8. E. Duregon *et al.*, Prolonged fasting times reap greater geroprotective effects when
599 combined with caloric restriction in adult female mice. *Cell Metab* **35**, 1179-1194 e1175
600 (2023).

601 9. V. A. Acosta-Rodriguez, M. H. M. de Groot, F. Rijo-Ferreira, C. B. Green, J. S. Takahashi,
602 Mice under Caloric Restriction Self-Impose a Temporal Restriction of Food Intake as
603 Revealed by an Automated Feeder System. *Cell Metab* **26**, 267-277 e262 (2017).

604 10. V. Acosta-Rodriguez *et al.*, Circadian alignment of early onset caloric restriction promotes
605 longevity in male C57BL/6J mice. *Science* **376**, 1192-1202 (2022).

606 11. H. Reinke, G. Asher, Crosstalk between metabolism and circadian clocks. *Nat Rev Mol*
607 *Cell Biol* **20**, 227-241 (2019).

608 12. I. Laothamatas, E. S. Rasmussen, C. B. Green, J. S. Takahashi, Metabolic and chemical
609 architecture of the mammalian circadian clock. *Cell Chem Biol* **30**, 1033-1052 (2023).

610 13. J. S. Takahashi, Transcriptional architecture of the mammalian circadian clock. *Nat Rev*
611 *Genet* **18**, 164-179 (2017).

612 14. G. Manella *et al.*, The liver-clock coordinates rhythmicity of peripheral tissues in response
613 to feeding. *Nat Metab* **3**, 829-842 (2021).

614 15. B. J. Greenwell *et al.*, Rhythmic Food Intake Drives Rhythmic Gene Expression More
615 Potently than the Hepatic Circadian Clock in Mice. *Cell Rep* **27**, 649-657 e645 (2019).

616 16. C. Vollmers *et al.*, Time of feeding and the intrinsic circadian clock drive rhythms in
617 hepatic gene expression. *Proc Natl Acad Sci U S A* **106**, 21453-21458 (2009).

618 17. K. A. Stokkan, S. Yamazaki, H. Tei, Y. Sakaki, M. Menaker, Entrainment of the circadian
619 clock in the liver by feeding. *Science* **291**, 490-493 (2001).

620 18. L. Palluth, J. S. Takahashi, C. B. Green, Keeping up with the nicotinamides: NADP(H),
621 the forgotten circadian cofactor that keeps metabolic time. *Life Metabolism*, loaf034
622 (2025).

623 19. S. Hood, S. Amir, The aging clock: circadian rhythms and later life. *J Clin Invest* **127**, 437-
624 446 (2017).

625 20. V. A. Acosta-Rodriguez, F. Rijo-Ferreira, C. B. Green, J. S. Takahashi, Importance of
626 circadian timing for aging and longevity. *Nat Commun* **12**, 2862 (2021).

627 21. A. Chaix, E. N. C. Manoogian, G. C. Melkani, S. Panda, Time-Restricted Eating to Prevent
628 and Manage Chronic Metabolic Diseases. *Annu Rev Nutr* **39**, 291-315 (2019).

629 22. W. E. Kraus *et al.*, 2 years of calorie restriction and cardiometabolic risk (CALERIE):
630 exploratory outcomes of a multicentre, phase 2, randomised controlled trial. *Lancet*
631 *Diabetes Endocrinol* **7**, 673-683 (2019).

632 23. V. D. Longo, S. Panda, Fasting, Circadian Rhythms, and Time-Restricted Feeding in
633 Healthy Lifespan. *Cell Metab* **23**, 1048-1059 (2016).

634 24. M. E. Parrotta *et al.*, Time Restricted Eating: A Valuable Alternative to Calorie Restriction
635 for Addressing Obesity? *Curr Obes Rep* **14**, 17 (2025).

636 25. D. M. Arble, J. Bass, A. D. Laposky, M. H. Vitaterna, F. W. Turek, Circadian timing of
637 food intake contributes to weight gain. *Obesity (Silver Spring)* **17**, 2100-2102 (2009).

638 26. E. N. C. Manoogian, L. S. Chow, P. R. Taub, B. Laferrere, S. Panda, Time-restricted Eating
639 for the Prevention and Management of Metabolic Diseases. *Endocr Rev* **43**, 405-436
640 (2022).

641 27. P. Balasubramanian *et al.*, Time-restricted feeding (TRF) for prevention of age-related
642 vascular cognitive impairment and dementia. *Ageing Res Rev* **64**, 101189 (2020).

643 28. S. Deota *et al.*, Diurnal transcriptome landscape of a multi-tissue response to time-
644 restricted feeding in mammals. *Cell Metab* **35**, 150-165 e154 (2023).

645 29. M. Hatori *et al.*, Time-restricted feeding without reducing caloric intake prevents metabolic
646 diseases in mice fed a high-fat diet. *Cell Metab* **15**, 848-860 (2012).

647 30. H. Sherman *et al.*, Timed high-fat diet resets circadian metabolism and prevents obesity.
648 *FASEB J* **26**, 3493-3502 (2012).

649 31. P. Regmi *et al.*, Early or delayed time-restricted feeding prevents metabolic impact of
650 obesity in mice. *J Endocrinol* **248**, 75-86 (2021).

651 32. C. Hepler *et al.*, Time-restricted feeding mitigates obesity through adipocyte
652 thermogenesis. *Science* **378**, 276-284 (2022).

653 33. E. N. C. Manoogian *et al.*, Feasibility of time-restricted eating and impacts on
654 cardiometabolic health in 24-h shift workers: The Healthy Heroes randomized control trial.
655 *Cell Metab* **34**, 1442-1456 e1447 (2022).

656 34. K. L. Haganes *et al.*, Time-restricted eating and exercise training improve HbA1c and body
657 composition in women with overweight/obesity: A randomized controlled trial. *Cell Metab*
658 **34**, 1457-1471 e1454 (2022).

659 35. T. Che *et al.*, Time-restricted feeding improves blood glucose and insulin sensitivity in
660 overweight patients with type 2 diabetes: a randomised controlled trial. *Nutr Metab (Lond)*
661 **18**, 88 (2021).

662 36. M. Dote-Montero *et al.*, Effects of early, late and self-selected time-restricted eating on
663 visceral adipose tissue and cardiometabolic health in participants with overweight or
664 obesity: a randomized controlled trial. *Nat Med* **31**, 524-533 (2025).

665 37. V. Pavlou *et al.*, Effect of Time-Restricted Eating on Weight Loss in Adults With Type 2
666 Diabetes: A Randomized Clinical Trial. *JAMA Netw Open* **6**, e2339337 (2023).

667 38. Z. Xie *et al.*, Randomized controlled trial for time-restricted eating in healthy volunteers
668 without obesity. *Nat Commun* **13**, 1003 (2022).

669 39. A. Chaix, A. Zarrinpar, P. Miu, S. Panda, Time-restricted feeding is a preventative and
670 therapeutic intervention against diverse nutritional challenges. *Cell Metab* **20**, 991-1005
671 (2014).

672 40. D. S. Whittaker *et al.*, Circadian modulation by time-restricted feeding rescues brain
673 pathology and improves memory in mouse models of Alzheimer's disease. *Cell Metab* **35**,
674 1704-1721 e1706 (2023).

675 41. A. Chaix, S. Deota, R. Bhardwaj, T. Lin, S. Panda, Sex- and age-dependent outcomes of
676 9-hour time-restricted feeding of a Western high-fat high-sucrose diet in C57BL/6J mice.
677 *Cell Rep* **36**, 109543 (2021).

678 42. M. Ulgherait *et al.*, Circadian autophagy drives iTRF-mediated longevity. *Nature* **598**, 353-
679 358 (2021).

680 43. K. Xie *et al.*, Every-other-day feeding extends lifespan but fails to delay many symptoms
681 of aging in mice. *Nat Commun* **8**, 155 (2017).

682 44. M. E. Starr, H. Saito, Age-related increase in food spilling by laboratory mice may lead to
683 significant overestimation of actual food consumption: implications for studies on dietary
684 restriction, metabolism, and dose calculations. *J Gerontol A Biol Sci Med Sci* **67**, 1043-
685 1048 (2012).

686 45. Y. D. Rathod, M. Di Fulvio, The feeding microstructure of male and female mice. *PLoS*
687 *One* **16**, e0246569 (2021).

688 46. K. Gabel *et al.*, Effects of 8-hour time restricted feeding on body weight and metabolic
689 disease risk factors in obese adults: A pilot study. *Nutr Healthy Aging* **4**, 345-353 (2018).

690 47. V. A. Acosta-Rodriguez *et al.*, Misaligned feeding uncouples daily rhythms within brown
691 adipose tissue and between peripheral clocks. *Cell Rep* **43**, 114523 (2024).

692 48. G. Manzanares, G. Brito-da-Silva, P. G. Gandra, Voluntary wheel running: patterns and
693 physiological effects in mice. *Braz J Med Biol Res* **52**, e7830 (2018).

694 49. V. S. Valentinuzzi, K. Scarbrough, J. S. Takahashi, F. W. Turek, Effects of aging on the
695 circadian rhythm of wheel-running activity in C57BL/6 mice. *Am J Physiol* **273**, R1957-
696 1964 (1997).

697 50. R. Garcia-Valles *et al.*, Life-long spontaneous exercise does not prolong lifespan but
698 improves health span in mice. *Longev Healthspan* **2**, 14 (2013).

699 51. O. Froy, Circadian aspects of energy metabolism and aging. *Ageing Res Rev* **12**, 931-940
700 (2013).

701 52. C. Lopez-Otin, L. Galluzzi, J. M. P. Freije, F. Madeo, G. Kroemer, Metabolic Control of
702 Longevity. *Cell* **166**, 802-821 (2016).

703 53. D. Gatfield, U. Schibler, Circadian glucose homeostasis requires compensatory
704 interference between brain and liver clocks. *Proc Natl Acad Sci U S A* **105**, 14753-14754
705 (2008).

706 54. D. L. Palliyaguru *et al.*, Fasting blood glucose as a predictor of mortality: Lost in
707 translation. *Cell Metab* **33**, 2189-2200 e2183 (2021).

708 55. J. C. Whitehead *et al.*, A clinical frailty index in aging mice: comparisons with frailty index
709 data in humans. *J Gerontol A Biol Sci Med Sci* **69**, 621-632 (2014).

710 56. J. Martinez-Romero *et al.*, A hematology-based clock derived from the Study of
711 Longitudinal Aging in Mice to estimate biological age. *Nat Aging* **4**, 1882-1896 (2024).

712 57. M. Magnani *et al.*, Effect of age on some properties of mice erythrocytes. *Mechanisms of*
713 *Ageing and Development* **42**, 37-47 (1988).

714 58. D. L. Palliyaguru, J. M. Moats, C. Di Germanio, M. Bernier, R. de Cabo, Frailty index as
715 a biomarker of lifespan and healthspan: Focus on pharmacological interventions. *Mech*
716 *Ageing Dev* **180**, 42-48 (2019).

717 59. D. W. Lamming, Quantification of healthspan in aging mice: introducing FAMY and
718 GRAIL. *Geroscience* **46**, 4203-4215 (2024).

719 60. R. Huang *et al.*, Multi-omics profiling reveals rhythmic liver function shaped by meal
720 timing. *Nat Commun* **14**, 6086 (2023).

721 61. J. S. Pendergast, K. L. Branecky, R. Huang, K. D. Niswender, S. Yamazaki, Wheel-running
722 activity modulates circadian organization and the daily rhythm of eating behavior. *Front*
723 *Psychol* **5**, 177 (2014).

724 62. A. M. Schroeder *et al.*, Voluntary scheduled exercise alters diurnal rhythms of behaviour,
725 physiology and gene expression in wild-type and vasoactive intestinal peptide-deficient
726 mice. *J Physiol* **590**, 6213-6226 (2012).

727 63. I. Janssen, S. B. Heymsfield, R. Ross, Low relative skeletal muscle mass (sarcopenia) in
728 older persons is associated with functional impairment and physical disability. *J Am*
729 *Geriatr Soc* **50**, 889-896 (2002).

730 64. E. Marzetti, C. Leeuwenburgh, Skeletal muscle apoptosis, sarcopenia and frailty at old age.
731 *Exp Gerontol* **41**, 1234-1238 (2006).

732 65. C. Livelo, Y. Guo, G. C. Melkani, A Skeletal Muscle-Centric View on Time-Restricted
733 Feeding and Obesity under Various Metabolic Challenges in Humans and Animals. *Int J*
734 *Mol Sci* **24**, (2022).

735 66. Y. O. Henderson *et al.*, Late-life intermittent fasting decreases aging-related frailty and
736 increases renal hydrogen sulfide production in a sexually dimorphic manner. *Geroscience*
737 **43**, 1527-1554 (2021).

738 67. Y. Yamada *et al.*, Caloric Restriction and Healthy Life Span: Frail Phenotype of
739 Nonhuman Primates in the Wisconsin National Primate Research Center Caloric
740 Restriction Study. *J Gerontol A Biol Sci Med Sci* **73**, 273-278 (2018).

741 68. O. Arum, Z. A. Rasche, D. J. Rickman, A. Bartke, Prevention of neuromusculoskeletal
742 frailty in slow-aging ames dwarf mice: longitudinal investigation of interaction of
743 longevity genes and caloric restriction. *PLoS One* **8**, e72255 (2013).

744 69. A. E. Kane *et al.*, Impact of Longevity Interventions on a Validated Mouse Clinical Frailty
745 Index. *J Gerontol A Biol Sci Med Sci* **71**, 333-339 (2016).

746 70. A. E. Kane *et al.*, Animal models of frailty: current applications in clinical research. *Clin*
747 *Interv Aging* **11**, 1519-1529 (2016).

748 71. R. Lok, J. Qian, S. L. Chellappa, Sex differences in sleep, circadian rhythms, and
749 metabolism: Implications for precision medicine. *Sleep Med Rev* **75**, 101926 (2024).

750 72. G. K. Paschos, R. Lordan, G. A. FitzGerald, Intersection of sex and circadian biology.
751 *Current Opinion in Physiology* **45**, 100834 (2025).

752 73. Z. Bahadoran, P. Mirmiran, K. Kashfi, A. Ghasemi, Effects of time-restricted feeding
753 (TRF)-model of intermittent fasting on adipose organ: a narrative review. *Eat Weight*
754 *Disord* **29**, 77 (2024).

755 74. P. Regmi, L. K. Heilbronn, Time-Restricted Eating: Benefits, Mechanisms, and Challenges
756 in Translation. *iScience* **23**, 101161 (2020).

757 75. P. Chen, B. Li, L. Ou-Yang, Role of estrogen receptors in health and disease. *Front*
758 *Endocrinol (Lausanne)* **13**, 839005 (2022).

759 76. V. M. Alvord, E. J. Kantra, J. S. Pendergast, Estrogens and the circadian system. *Semin*
760 *Cell Dev Biol* **126**, 56-65 (2022).

761 77. K. M. Hatcher, S. E. Royston, M. M. Mahoney, Modulation of circadian rhythms through
762 estrogen receptor signaling. *Eur J Neurosci* **51**, 217-228 (2020).

763 78. L. Zhu *et al.*, Estrogens prevent metabolic dysfunctions induced by circadian disruptions
764 in female mice. *Endocrinology* **156**, 2114-2123 (2015).

765 79. L. Talamanca, C. Gobet, F. Naef, Sex-dimorphic and age-dependent organization of 24-
766 hour gene expression rhythms in humans. *Science* **379**, 478-483 (2023).

767 80. J. A. Krizo, E. M. Mintz, Sex differences in behavioral circadian rhythms in laboratory
768 rodents. *Front Endocrinol (Lausanne)* **5**, 234 (2014).

769 81. A. A. Astafev, V. Mezhnina, A. Poe, P. Jiang, R. V. Kondratov, Sexual dimorphism of
770 circadian liver transcriptome. *iScience* **27**, 109483 (2024).

771 82. S. J. Mitchell *et al.*, Effects of Sex, Strain, and Energy Intake on Hallmarks of Aging in
772 Mice. *Cell Metab* **23**, 1093-1112 (2016).

773 83. A. E. Kane, D. A. Sinclair, J. R. Mitchell, S. J. Mitchell, Sex differences in the response to
774 dietary restriction in rodents. *Curr Opin Physiol* **6**, 28-34 (2018).

775 84. J. F. Lemaitre *et al.*, Sex differences in adult lifespan and aging rates of mortality across
776 wild mammals. *Proc Natl Acad Sci U S A* **117**, 8546-8553 (2020).

777 85. S. N. Austad, K. E. Fischer, Sex Differences in Lifespan. *Cell Metab* **23**, 1022-1033 (2016).

778 86. D. E. Harrison *et al.*, Acarbose, 17-alpha-estradiol, and nordihydroguaiaretic acid extend
779 mouse lifespan preferentially in males. *Aging Cell* **13**, 273-282 (2014).

780 87. R. A. Miller *et al.*, Rapamycin, but not resveratrol or simvastatin, extends life span of
781 genetically heterogeneous mice. *J Gerontol A Biol Sci Med Sci* **66**, 191-201 (2011).

782 88. R. Strong *et al.*, Nordihydroguaiaretic acid and aspirin increase lifespan of genetically
783 heterogeneous male mice. *Aging Cell* **7**, 641-650 (2008).

784 89. B. N. Gaskill *et al.*, Impact of nesting material on mouse body temperature and physiology.
785 *Physiol Behav* **110-111**, 87-95 (2013).

786 90. K. Kaikaew, J. Steenbergen, A. P. N. Themmen, J. A. Visser, A. Grefhorst, Sex difference
787 in thermal preference of adult mice does not depend on presence of the gonads. *Biol Sex*
788 *Differ* **8**, 24 (2017).

789 91. K. Kaikaew *et al.*, Sex difference in cold perception and shivering onset upon gradual cold
790 exposure. *J Therm Biol* **77**, 137-144 (2018).

791 92. C. Fernandez-Pena, A. Reimundez, F. Viana, V. M. Arce, R. Senaris, Sex differences in
792 thermoregulation in mammals: Implications for energy homeostasis. *Front Endocrinol*
793 *(Lausanne)* **14**, 1093376 (2023).

794 93. Z. Zhao *et al.*, Body temperature is a more important modulator of lifespan than metabolic
795 rate in two small mammals. *Nat Metab* **4**, 320-326 (2022).

796 94. B. Conti *et al.*, Transgenic mice with a reduced core body temperature have an increased
797 life span. *Science* **314**, 825-828 (2006).

798 95. A. W. Fischer, B. Cannon, J. Nedergaard, Optimal housing temperatures for mice to mimic
799 the thermal environment of humans: An experimental study. *Mol Metab* **7**, 161-170 (2018).

800 96. C. L. Karp, Unstressing intemperate models: how cold stress undermines mouse modeling.
801 *J Exp Med* **209**, 1069-1074 (2012).

802 97. A. L. Ray *et al.*, The role of sex in the innate and adaptive immune environment of
803 metastatic colorectal cancer. *Br J Cancer* **123**, 624-632 (2020).

804 98. E. G. Vichaya *et al.*, Sex differences in the behavioral and immune responses of mice to
805 tumor growth and cancer therapy. *Brain Behav Immun* **98**, 161-172 (2021).

806 99. J. B. Rubin, The spectrum of sex differences in cancer. *Trends Cancer* **8**, 303-315 (2022).

807 100. M. K. E. Ougaard *et al.*, Murine Nephrotoxic Nephritis as a Model of Chronic Kidney
808 Disease. *Int J Nephrol* **2018**, 8424502 (2018).

809 101. United States Renal Data System. (National Institute of Diabetes and Digestive and Kidney
810 Diseases, National Institutes of Health, Bethesda, MD).

811 102. G. J. Shim, L. L. Kis, M. Warner, J. A. Gustafsson, Autoimmune glomerulonephritis with
812 spontaneous formation of splenic germinal centers in mice lacking the estrogen receptor
813 alpha gene. *Proc Natl Acad Sci U S A* **101**, 1720-1724 (2004).

814 103. J. H. Catterson *et al.*, Short-Term, Intermittent Fasting Induces Long-Lasting Gut Health
815 and TOR-Independent Lifespan Extension. *Curr Biol* **28**, 1714-1724 e1714 (2018).

816 104. Y. Yang, D. Liu, Impacts of time-restricted feeding on middle-aged and old mice with
817 obesity. *J Physiol*, (2024).

818 105. P. Domaszewski *et al.*, Effect of a six-week times restricted eating intervention on the body
819 composition in early elderly men with overweight. *Sci Rep* **12**, 9816 (2022).

820 106. O. Hahn *et al.*, A nutritional memory effect counteracts benefits of dietary restriction in
821 old mice. *Nat Metab* **1**, 1059-1073 (2019).

822 107. A. C. Hofacker, M. Knop, S. Krauss-Etschmann, T. Roeder, Time-Restricted Feeding
823 Promotes Longevity and Gut Health Without Fitness Trade-Offs. *FASEB J* **39**, e70627
824 (2025).

825 108. M. J. Schafer *et al.*, Late-life time-restricted feeding and exercise differentially alter
826 healthspan in obesity. *Aging Cell* **18**, e12966 (2019).

827 109. M. Das *et al.*, Time-Restricted Feeding Attenuates Metabolic Dysfunction-Associated
828 Steatohepatitis and Hepatocellular Carcinoma in Obese Male Mice. *Cancers (Basel)* **16**,
829 (2024).

830 110. E. B. Parr, B. L. Devlin, B. E. Radford, J. A. Hawley, A Delayed Morning and Earlier
831 Evening Time-Restricted Feeding Protocol for Improving Glycemic Control and Dietary
832 Adherence in Men with Overweight/Obesity: A Randomized Controlled Trial. *Nutrients*
833 **12**, (2020).

111. K. Gabel, S. Cienfuegos, F. Kalam, M. Ezpeleta, K. A. Varady, Time-Restricted Eating to Improve Cardiovascular Health. *Curr Atheroscler Rep* **23**, 22 (2021).

112. P. Pati *et al.*, Time-restricted feeding reduces cardiovascular disease risk in obese mice. *JCI Insight* **10**, (2025).

113. M. Milan *et al.*, Time-restricted feeding improves aortic endothelial relaxation by enhancing mitochondrial function and attenuating oxidative stress in aged mice. *Redox Biol* **73**, 103189 (2024).

114. R. A. Miller *et al.*, Glycine supplementation extends lifespan of male and female mice. *Aging Cell* **18**, e12953 (2019).

115. N. Ogiso *et al.*, Biological characteristics of age-related changes in C57BL/6 mice sub-strains in the national center for geriatrics and gerontology aging farm. *Exp Anim* **74**, 229-238 (2025).

116. W. J. Schwartz, P. Zimmerman, Circadian timekeeping in BALB/c and C57BL/6 inbred mouse strains. *J Neurosci* **10**, 3685-3694 (1990).

117. M. Pfeffer, C. von Gall, H. Wicht, H. W. Korf, The Role of the Melatoninergic System in Circadian and Seasonal Rhythms-Insights From Different Mouse Strains. *Front Physiol* **13**, 883637 (2022).

118. G. Banks *et al.*, Genetic background influences age-related decline in visual and nonvisual retinal responses, circadian rhythms, and sleep. *Neurobiol Aging* **36**, 380-393 (2015).

119. S. M. Siepka, J. S. Takahashi, Methods to record circadian rhythm wheel running activity in mice. *Methods Enzymol* **393**, 230-239 (2005).

120. A. A. Bachmanov, D. R. Reed, G. K. Beauchamp, M. G. Tordoff, Food intake, water intake, and drinking spout side preference of 28 mouse strains. *Behav Genet* **32**, 435-443 (2002).

121. D. R. Reed, A. A. Bachmanov, M. G. Tordoff, Forty mouse strain survey of body composition. *Physiol Behav* **91**, 593-600 (2007).

122. J. W. Cooley, J. W. Tukey, An Algorithm for the Machine Calculation of Complex Fourier Series. *Mathematics of Computation* **19**, 297-301 (1965).

123. R. B. Blackman, J. W. Tukey, The measurement of power spectra from the point of view of communications engineering — Part I. *The Bell System Technical Journal* **37**, 185-282 (1958).

124. C. Wang, Q. Li, D. T. Redden, R. Weindruch, D. B. Allison, Statistical methods for testing effects on "maximum lifespan". *Mech Ageing Dev* **125**, 629-632 (2004).

Acknowledgements: Thanks to G. Martinez, K. Brown, C. Joseph, G. Flowers, A. Torres, A. Herrera, R. Lewis, and L. Thomas, for assisting with the mouse husbandry and experiments. To S. McPherson, K. Goedde, K. Auldridge, and S. Elias Perryman of the Animal Resource Center

871 Diagnostics Lab for their assistance with the gross necropsies. To veterinarians Dr. S. Lewis and
872 Dr. C. Jones for providing guidance on mouse health care. To S. Dixon for providing
873 administrative support. Additional thanks to M. Wellems at Phenome Technologies and D. Ferster
874 at Actimetrics for the feeders and software system. This work was supported by the Howard
875 Hughes Medical Institute awarded to JST, the National Institute of Health (NIH/NIA AG045795
876 to JST and CBG; NIH/NIA AG072736 to JST and CBG; NIH/NIGMS GM127122 to CBG; NIH
877 1T32HL138438 to JST and SEI), and the Milky Way Research Foundation MWRF210823
878 awarded to JST and CBG.

879 This research was supported in part by the Intramural Research Program of the National Institutes
880 of Health (NIH). The contributions of the NIH author(s) were made as part of their official duties
881 as NIH federal employees, are in compliance with agency policy requirements, and are considered
882 Works of the United States Government. However, the findings and conclusions presented in this
883 paper are those of the author(s) and do not necessarily reflect the views of the NIH or the U.S.
884 Department of Health and Human Services.

885

886 **Author Contributions:** SEI, NJS, VAR, CBG, and JST conceptualized the study, developed the
887 experimental design, and oversaw all aspects of project execution and supervision. MW-C
888 performed all histopathological assessments and interpretations. SEI, NJS, and VAR conducted all
889 remaining experimental work, including animal handling, data curation, and statistical analyses.
890 SEI, NJS, VAR, CBG, and JST wrote and revised the manuscript with additional edits from MW-
891 C. Funding acquisition was provided by CBG and JST.

892

893 **Competing interests:** The authors declare no competing interests.

894

895 **Data and materials availability:** Data are available in the main text or the supplementary
896 materials

897

898 **Supplementary Materials:**

899 Materials and Methods

900 Figures S1 to S17

901 Tables S1 to S7

902

903 **Materials and Methods:**

904 **Animals and Housing Conditions**

905 For a minimum detection of 10% life extension with 80% power a minimum of 96 animals were
906 needed in the control group and 72 in each of the two TRF groups (*114*). Extra mice were included
907 in each group to account for any that may not adapt to the feeder/diet or for non-aging-related
908 deaths.

909 264 male and 264 female C57BL/6J mice 6 weeks of age were ordered from Jackson Laboratories,
910 Bar Harbor, ME. We selected C57BL/6J mice because they are widely used research model which
911 exhibit robust circadian rhythms and well-known aging phenotypes (*115-118*). Further, using a
912 single, well-characterized strain maximized statistical power and lifespan resolution in our large
913 cohort (*114*). As done previously, starting at 2 months of age the mice were: **(i)** individually housed
914 in standard polycarbonate cages with stainless steel running wheels inside isolation cabinets under

915 light:dark (LD) of 12:12 hours and ambient building temperature 72-78ºF, **(ii)** fed 300mg pellets
916 of purified diet (F0075, Bio-Serv) using automated feeders with water provided *ad libitum* (AL),
917 and **(iii)** cage changed every 21 days (*9, 10, 119*). Nesting material and igloos were excluded,
918 besides shavings, to prevent wheel blockages. The Institutional Animal Care and Use Committee
919 (IACUC) of the University of Texas Southwestern Medical Center approved the animal protocol
920 (APN 2015-100925), which has been renewed every 3 years (in 2018, 2021, and 2024).

921 The purified diet (F0075, Bio-Serv) is composed of 18.7% protein, 5.6% fat, 4.7% fiber, and 59.1%
922 carbohydrates, similar to regular mouse chows. Major ingredients include Sucrose. Dextrose,
923 Casein, Corn Oil, Mineral Mix, Cellulose, Corn Syrup, Calcium Silicate, Vitamin Mix,
924 Magnesium Stearate, Choline Bitartrate, DL-Methionine, L-Cystine, Ascorbic Acid, Vitamin E
925 Acetate, and tBHQ.

926 An additional cohort of C57BL/6J animals (N=48/feeding condition/sex) were included in this
927 study in order to undergo more invasive assays. These mice were randomly selected (N=8-
928 12/group/age point) for analysis of metabolism in metabolic chambers, fasting blood glucose
929 levels, glucose tolerance, biomarkers of inflammation and metabolism and hematology. These
930 mice were not included in the longitudinal health measurements or the assessment of lifespan.

931

932 **Time-Restricted Feeding (TRF) Regimens**

933 At 2 months of age, unmated mice were placed in individual cages as described above and fed *ad*
934 *libitum* (AL) for 8 weeks using the automated feeder system (*9, 10*). At 4 months of age, the mice
935 were divided into three feeding groups for the remainder of the experiment: **(i)** 108 of each sex
936 continued in AL as a control group, **(ii)** 78 of each sex in a 12-hour TRF group where the automated

937 feeder restricted food dispensing to the 12-hour night (12h-TRF, ZT12-24), and **(iii)** 78 of each
938 sex in an 8-hour TRF group with food dispensing restricted to the middle 8 hours of the night (8h-
939 TRF, ZT14-22). These feeding windows were chosen as they have been previously validated and
940 demonstrated to confer health benefits in mice (*25, 29*). In addition to the timing of the feeding
941 window, the feeders were also programmed with a 10-minute delay between pellet dispensing to
942 reduce hoarding behavior. Regardless of the feeding group, all mice had access to a maximum of
943 22 pellets/day or 6.6 g of food. In this study, no group exceeded 6.6 g daily consumption. Previous
944 studies have shown that C57BL/6J mice consume 4-5g of food per day (*120*), so this amount of
945 food was chosen to ensure mice were not calorically restricted.

946

947 **Exclusion of Hoarded Food**

948 Mice exhibit a natural tendency to hoard food within the cage, especially later in life or when ill
949 (*44*). In all TRF groups, mice identified as hoarders were flagged, and hoarded food was removed
950 from the cage on a weekly basis. For mice on veterinary health report, hoarded food was removed
951 at their twice weekly full health check. The total amount of hoarded food was quantified by weight
952 (g) at each 21-day cage change. For AL mice, hoarded food was allowed to remain in the cage
953 until the scheduled cage change, at which point it was collected and quantified. In all groups, the
954 total hoarded food weight was divided by 21 days to estimate an average daily hoarding amount,
955 which was then subtracted from the average daily food retrieval recorded by the feeder.

956

957 **Daily Monitoring of Feeding and Wheel-Running Activity**

958 As before, the feeders were set and continuously recorded quantity and timing of food intake via
959 ClockLab Chamber Control Software v3.401 (Actimetrics Inc., Wilmette, IL, USA) (*9, 10*). The
960 feeding data presented in Figure 1B and Supplemental figures S2 and S3 represent food
961 consumption with hoarding removed. All other feeding figures represent the quantity and pattern
962 of pellet taking from the feeder, not excluding hoarded food. Wheel-running activity was also
963 continuously recorded as before using an updated version of ClockLab Data Acquisition System
964 v3.604 (Actimetrics Inc., Wilmette, IL, USA).

965

966 **Body Weight and Composition Measurements**

967 The body weight of each mouse was measured every 21 days during cage change (morning, ZT4-
968 7) throughout its lifespan. Body composition measurements of lean and fat mass (g) were assessed
969 every 6 months during cage change (ZT4-7) using a 100H-EchoMRI Body Composition Analyzer
970 (EchoMRI, Houston, TX, USA).

971

972 **Promethion Metabolic Chambers**

973 These tests were performed in a follow-up cohort of mice. Mice were randomly selected.

974 At 19 months of age, mice received body composition measurements (EchoMRI) and then were
975 individually housed in metabolic cages (Promethion, Sable Systems International) modified with
976 automated feeders to maintain the same feeding regimens. These cages were housed in light-tight,
977 temperature-controlled cabinets. Mice were acclimatized for 2-3 days at room temperature (25°C)
978 before recording for an additional 5-6 days at room temperature. Cabinet temperature was then
979 raised to thermoneutrality (30°C) for 5 days.

980

981 **Fasting Glucose and Glucose Tolerance Testing**

982 These tests were performed in a follow-up cohort of mice. Mice were randomly selected from the
983 cohort at each age point.

984 For fasting glucose, cages for all mice to be tested were changed out fresh the day before. Feeders
985 for all groups were shut off at ZT21.5 to allow the mice 30 minutes to consume the last pellet
986 dropped and officially begin their 12h fast at ZT22. Mice were checked again at ZT0 to ensure no
987 pellets remained in the cage or available in the pellet chute. At ZT10, a drop of blood was measured
988 from the tail using an Accu-Check Glucose Meter.

989 For glucose tolerance testing, cages were changed fresh and mice fasted as described above. At
990 ZT10, mice were injected with a 20% glucose solution at a dose of 0.1mL per 25g of body weight.
991 A drop of blood from the tail was measured for glucose at the time of injection (0 min) and then
992 at 15-, 30-, 45-, 60-, and 120-min post-injection.

993

994 **Biomarkers of Metabolism and Inflammation**

995 These markers were measured in a follow-up cohort of mice. Mice were randomly selected from
996 the cohort at each age point.

997 Mice were switched to fresh cages and were fasted for 12h as described above for fasting glucose.
998 At ZT10, 70-100μL of blood was collected via submandibular bleed into K_2 EDTA coated
999 collection tubes (RAM Scientific Safe-T-Fill™ Capillary Blood Collection Systems) with
1000 cOmplete™, Mini, EDTA-free Protease Inhibitor Cocktail (Roche) and DPP-IV (Millipore).

1001 Blood was immediately kept on ice and then spun down at 2000g for 10 min at 4ºC. The upper
1002 layer of plasma was transferred to a new tube and stored at -80ºC until use.

1003 20-25µL of plasma was then measured for leptin, insulin, IL-1β, IL-6, IL-10, TNFα, MCP-1, and
1004 BDNF using a U-PLEX Adipokine Combo 1 (mouse) assay kit (Meso Scale Discovery).

1005

1006 **Hematology**

1007 Measurements for red blood cells, white blood cells, and platelets were performed in a follow-up
1008 cohort of mice. Mice were randomly selected from the cohort at each age point.

1009 Mice were switched to fresh cages and were fasted for 12h as described above for fasting glucose.
1010 At ZT10, 25-30µL of blood was collected via submandibular bleed into K_2 EDTA coated
1011 collection tubes (RAM Scientific Safe-T-Fill™ Capillary Blood Collection Systems) with
1012 cOmplete™, Mini, EDTA-free Protease Inhibitor Cocktail (Roche) and DPP-IV (Millipore). 20µL
1013 of whole blood was then measured in a Hemavet 950FS (Drew Scientific) at room temperature
1014 within 2-4 hours of collection.

1015

1016 **Frailty Scoring**

1017 Every 6 months the mice were assessed for frailty, or physical vulnerabilities, according to 31
1018 parameters of aging modified from Whitehead et al. 2014 (*55*). These parameters include a range
1019 of physiological evaluations, scoring coat condition, ocular and auditory responses, physical and
1020 musculoskeletal state, respiration rate, body weight, and temperature. Each assessment was scored
1021 either 0=absent, 0.5=mild, or 1=severe. For scoring Body Condition Scores, 0.5 was used for either
1022 a BCS of 2 or 4, and 1 was for a BCS of 1 or 5. For body weight and body temperature scores only,

1023 these were determined by averaging the group measurements and then determining how many
1024 standard deviations (SD) each individual mouse was from their age-, sex- and feeding-matched
1025 group mean. If <1 SD, mouse scored as 0 for that parameter, 1-1.99 SD = 0.25, 2-2.99 SD = 0.5,
1026 3-3.99 = 0.75, and >4 SD = 1. The scores were totaled to calculate an overall index score.

1027

1028 **Health Monitoring and Survival Study**

1029 Mice were physically health checked every 21 days during cage change and visually inspected
1030 every 10 days during refilling of the automated feeders. Using the feeding and wheel monitoring
1031 software, mice were also checked virtually every day and only physically health checked if feeding
1032 fell to <5 pellets per/day and/or wheel running fell below set thresholds (1.14 counts/min within
1033 24hr, reduced by 10% every 6 months as the mice age) as performed previously (*10*).

1034 If any mouse was found to have a mild/moderate health ailment (e.g. dermatitis, external tumor,
1035 abdominal mass, head tilt) or a body condition score < 3 (Scored 1-5 with: 1 being emaciated, 3
1036 ideal condition, and 5 obese) it was placed on veterinary health report. These records were also
1037 used to generate Figures 4D-F. Mice on health report were physically health checked weekly by
1038 the UT Southwestern Animal Resource Facility (ARC) veterinary staff and twice a week by our
1039 own laboratory staff. In order to obtain accurate but humane lifespan data, mice were monitored
1040 carefully for euthanasia criteria that would indicate imminent death (moribund) or unacceptable
1041 levels of pain (analgesics were not used to avoid confounding lifespan results). Criteria were
1042 determined in conjunction with the ARC veterinarians according to AAALAC guidelines and
1043 include: Non-responsive to touch, hypothermic or cold to touch, slow or labored breathing, failure
1044 or inability to eat/drink after moist chow is given, a body condition score of 1, body weight loss
1045 of >20% from baseline or between cage changes, a broken/fractured/dislocated limb, head tilt that

1046 is resulting in an animal being unable to maintain sternal body position which would affect their
1047 ability to consume food and water, severe eye protrusion/infection, severe dermatitis, grade 3 rectal
1048 or penile prolapse, urinary obstruction, or a subcutaneous tumor >2cm.

1049 The number and date of those euthanized or found dead across the feeding groups and sexes were
1050 recorded and used to generate the Kaplan-Meier survival curves. A total of 35 animals (35/528)
1051 were censored from the survival curve if death occurred earlier than 6 months or due to non-aging
1052 related injuries or death: 9 AL females, 6 12h-TRF females, 6 8h-TRF females, 9 AL males and 5
1053 8h-TRF males.

1054

1055 **Necropsy and Histopathology**

1056 Mice euthanized or found dead were submitted for gross necropsy and blinded histopathological
1057 analysis was performed, as done previously (*10*). Less than 10% of the animals submitted were
1058 too autolyzed to analyze. Disease types were tallied together by tissue type, sex, and feeding group.

1059

1060 **Healthspan Index**

1061 Throughout the experiment we recorded thirteen health measures including: wheel-running
1062 activity to determine overall activity level and diurnal amplitude, food consumption to determine
1063 overall level and diurnal amplitude**,** 90% feeding duration, maximum fasting times, body weight,
1064 composition of lean and fat mass as a percentage of body weight, body condition score, frailty
1065 index, and the onset and duration of veterinary health reports.

1066 Healthspan index was calculated by summing the calculated scaled values of each of the thirteen
1067 health measures. In the case of body condition score, an absolute difference from BCS=3 was

1068 calculated. For body fat percentage, an absolute difference in value from 24.45% was calculated.
1069 The value 24.45% was used based on previous literature showing the average body fat percentage
1070 across multiple healthy mouse strains at the age of 16 weeks (*121*). All measures were then
1071 normalized to a mean of 0 and a standard deviation of 1, within each measure. Certain values were
1072 then inverted, given their context, in order to have positive numbers representing a healthier state,
1073 and negative values representing an unhealthy state. For example, "Days on Health Report" is
1074 inverted, as higher values would be less healthy, and lower values are healthier. All normalized
1075 values were then summed together at 21-day intervals.

1076

1077 **FAMY**

1078 FAMY was calculated using the lifetime of frailty scores collected for each mouse and as described
1079 in Lamming 2024 (*59*).

1080

1081 **Statistical Analyses**

1082 All measurements represent repeated measures from the same animals over time, with the
1083 exception of data shown in Figs. S7–S10 and S13–S15, which were collected from a separate
1084 cohort using different mice at each age point. Sample sizes (N) for each experiment are indicated
1085 in the corresponding figure legends.

1086 As performed previously, all feeding and wheel-running activity was collected using Chamber
1087 Control and ClockLab, respectively (Actimetrics, Inc) (*10*). Each point on the longitudinal profiles
1088 represents a 21-day mean. 24h profiles were binned by hour, with each age point reflecting a 14-
1089 day mean (taken from the middle of each 21-day cage cycle to avoid behavioral changes due to

cage change stress). For each mouse, each 14-day bin was then analyzed by 1-dimensional Discrete Fast Fourier Transform (FFT) using the mixed-radix algorithm for real-valued input (SciPy v1.12.0; scipy.fft.rfft) (*122*). The Blackman window function is applied to the data prior to FFT analysis to inhibit spectral leakage (*123*). The power of each frequency component is then normalized, with the total normalized power of all frequency components equaling 100. The normalized power from the 24h frequency component is then taken as the diurnal amplitude of either food intake behavior or running wheel activity. This value represents the percentage of contribution of the 24h frequency component, to the entire 14-day behavioral period. For example, if the diurnal amplitude for food intake is 21, it indicates that 21% of the observed variation in food intake can be directly attributed to the animal's consistent 24-hour daily cycle. Group-wise statistics were then performed to determine the overarching impact of each intervention, as described below.

For the calculation of the 90% feeding window, food intake data was similarly partitioned into 3-week intervals, with each sampling point consisting of a 14-day window. Only windows containing a minimum of 84 feeding events (averaging 6 events per day, or ~1.8g of intake) were included in the final density analysis to ensure robust statistical estimation. Because time-of-day is a periodic variable, we employed a von Mises distribution (the circular analogue of the Normal distribution) to estimate the probability density of feeding activity. We utilized the vonmises.pdf method (SciPy v1.12.0), to compute the circular distribution, where the concentration parameter κ, was defined by a fixed bandwidth of 0.04363 radians, representing approximately 10 minutes of smoothing. To define the primary feeding window, we identified the shortest continuous arc on the circle containing 90% of the total probability mass. This method accounts for feeding windows that cross over the ZT24/ZT0 boundary.

Cumulative health report and survival curves were analyzed using Log-rank Mantel Cox and Fisher's exact test, health report type and necropsy report disease type percentages analyzed by contingency tables and Fisher's exact test and, and all other plots analyzed using two-way ANOVA or type III ANOVA with Tukey's or Holm's post-hoc analyses (*124*). All statistical tests were two-sided. Normality was assumed but not formally tested. Data plots were generated and statistically analyzed by Prism 10 (Graphpad Software Inc), Python, and R software, using custom-written scripts and standard libraries.

1120 **Supplemental Figures and Legends:**

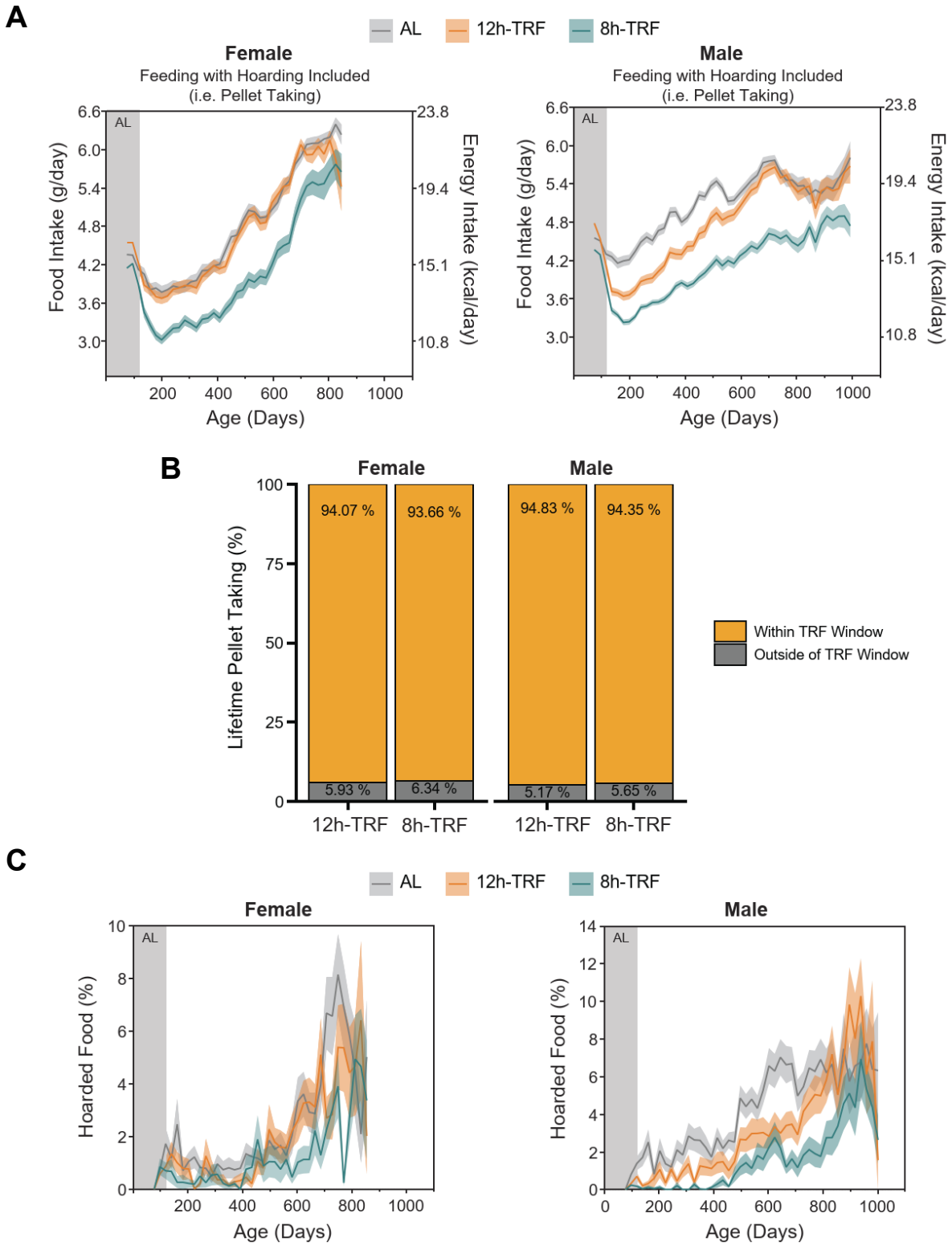

1121 **Figure S1: Food taking and hoarding behavior:** 300mg pellets are dispensed from the feeder
1122 one at a time for the mouse to retrieve. In females and males: (**A**) Longitudinal profiles of daily
1123 food taken from the feeder including uneaten (hoarded) food found in the cage (g/day) and the
1124 equivalent energy intake (kcal/day). (**B**) Lifetime averages of the percent (%) of food taken from
1125 the feeder within or outside of the TRF window. (**C**) Longitudinal profiles of hoarded food
1126 removed from cages as a % of the total food taken from the feeder. A and C: *Ad libitum* (AL)
1127 baseline feeding (Gray area). Time-restricted feeding (TRF) (White area). Mean of 21 days ± SEM
1128 (shaded regions). Females N=71-103 per group. Males N=71-97 per group.

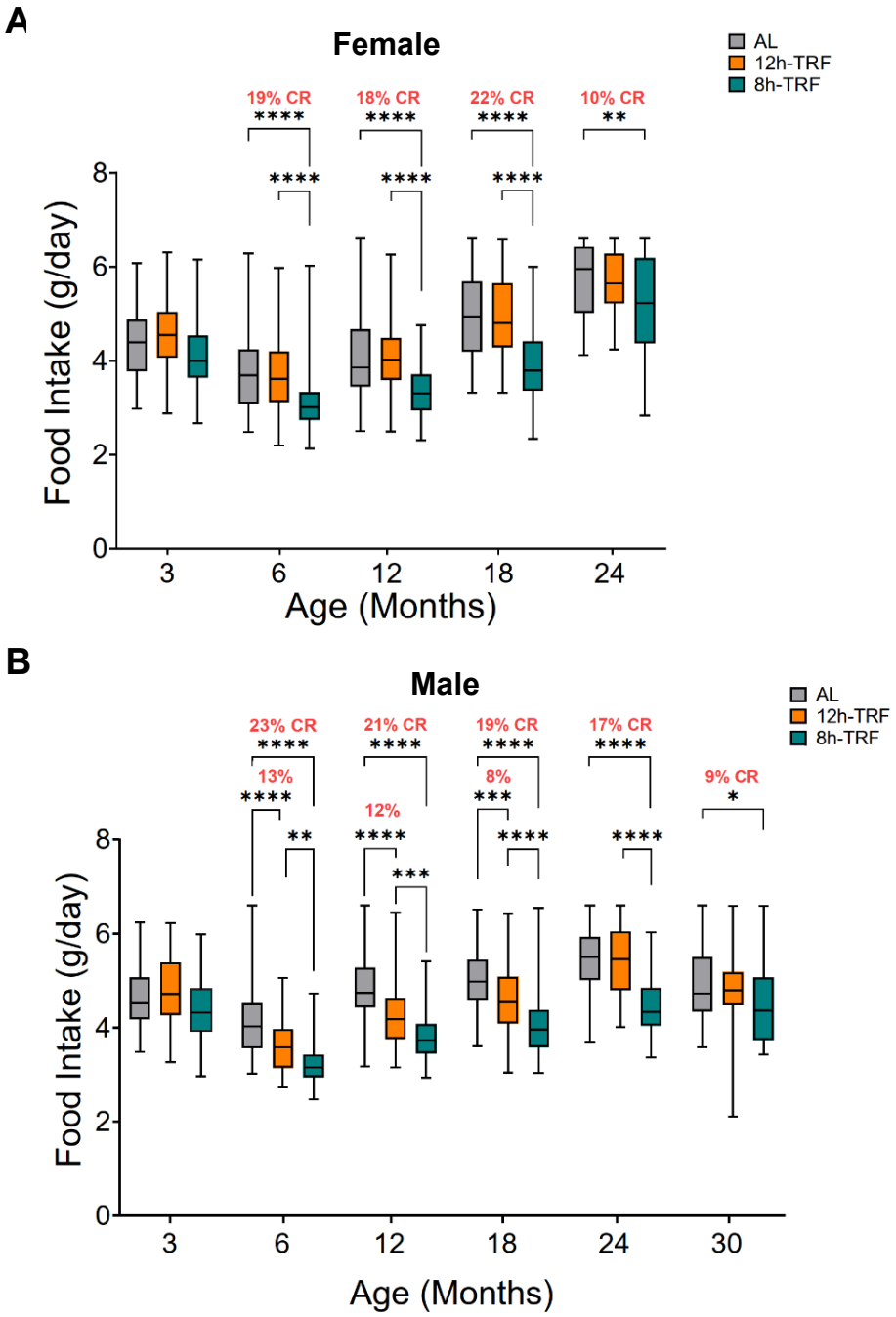

1129 **Figure S2: Food intake by monthly age epochs:** (**A**) In females and (**B**) males, box plots of food
1130 intake with hoarding removed (g/day) at 3 and 6 months of age and then every 6 months following.
1131 Food intake per mouse averaged every 21 days. Any caloric restriction (CR) relative to the AL
1132 control at each age epoch shown as %. Two-way ANOVA, Tukey's post-hoc. *P ≤ 0.05; **P ≤
1133 0.01; ***P ≤ 0.001; ****P ≤0.0001.

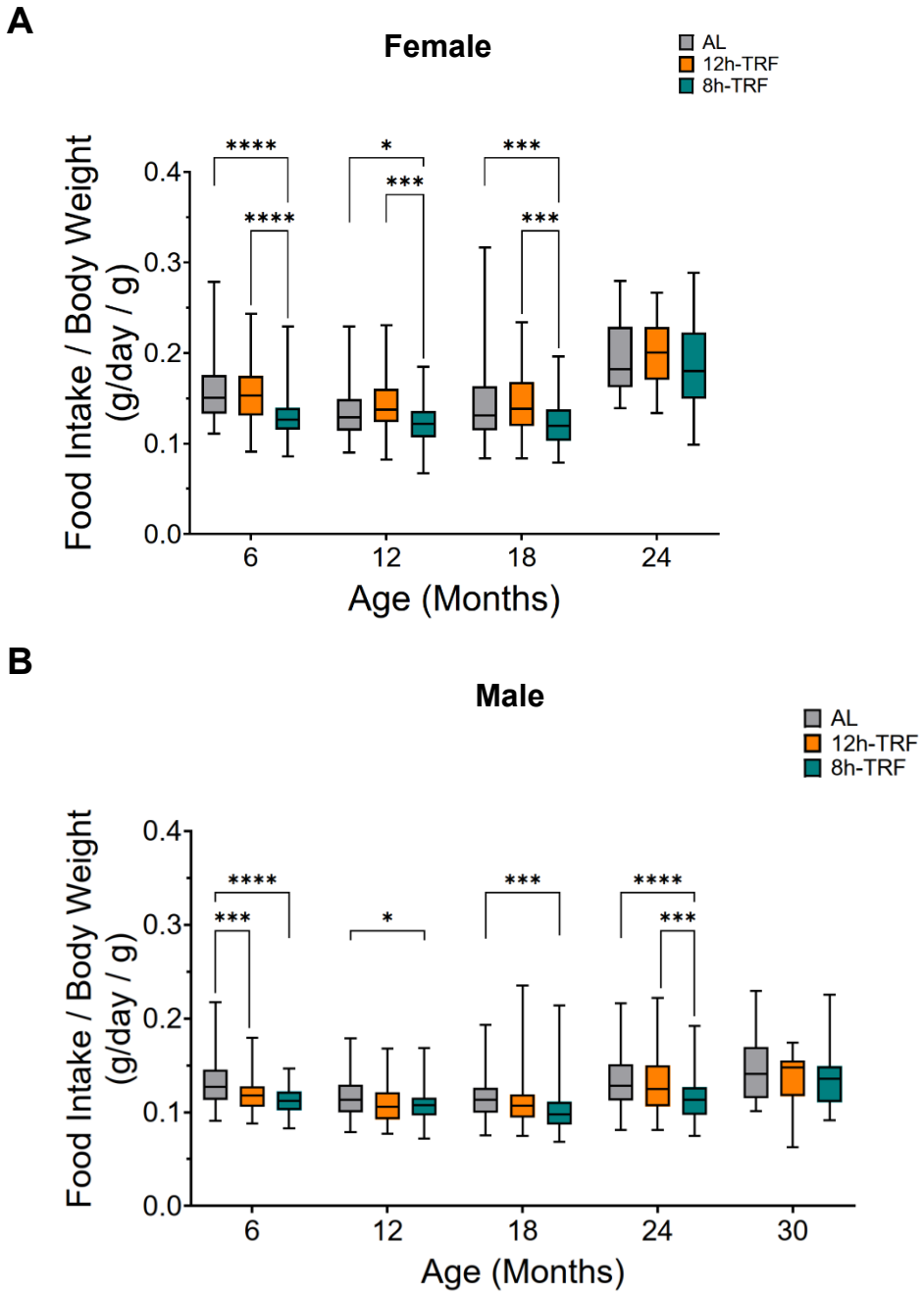

Figure S3: Food intake relative to body weight by monthly age epochs: (**A**) In females and (**B**) males, boxplots of food intake (g/day) with hoarding removed relative to body weight (g) at 6 months of age and then every 6 months following. Two-way ANOVA, Tukey's post-hoc. *P ≤ 0.05; **P ≤ 0.01; ***P ≤ 0.001; ****P ≤0.0001.

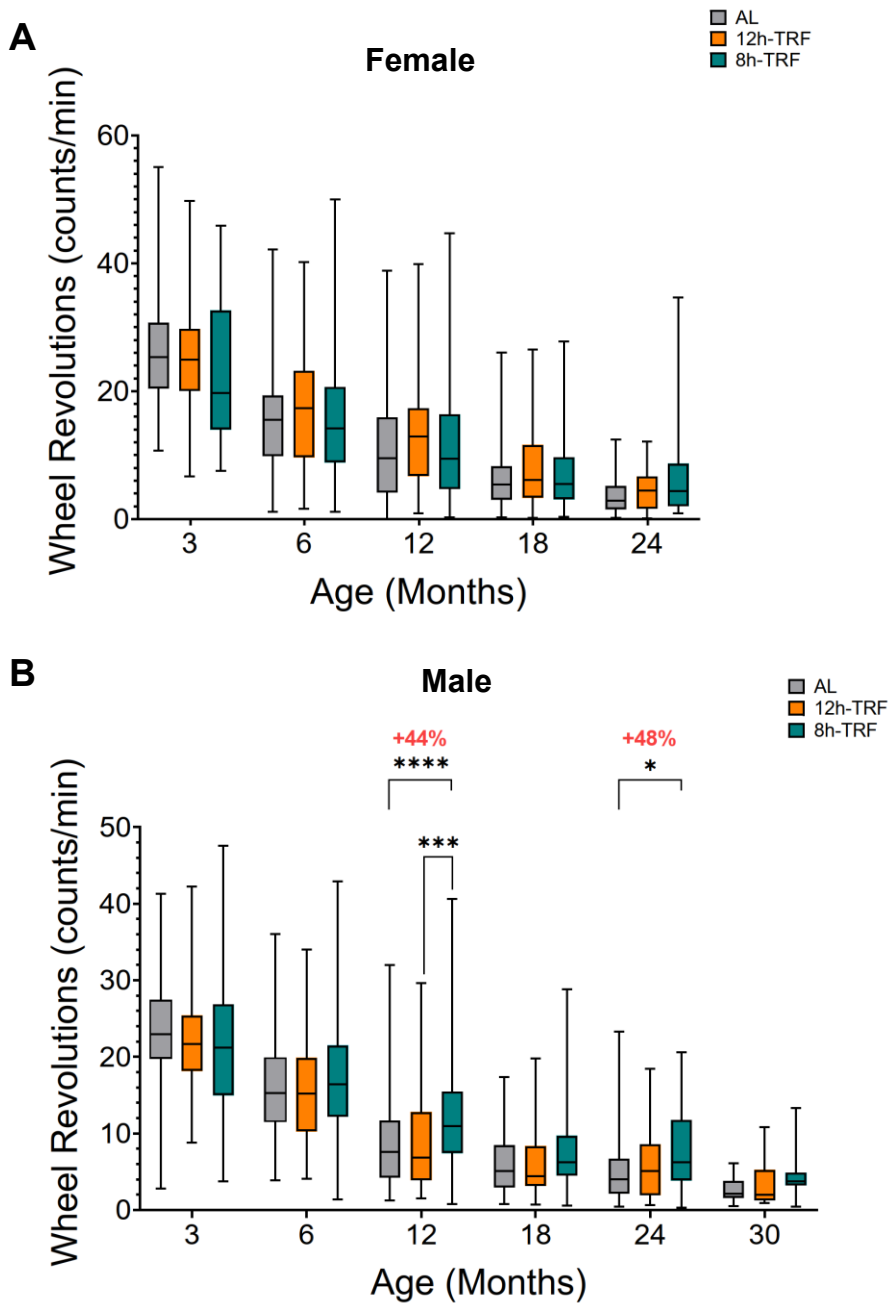

Figure S4: Wheel activity by monthly age epochs: (**A**) In females and (**B**) males, boxplots of daily wheel revolutions (counts/min) at 3 and 6 months of age and then every 6 months following. Wheel running per mouse averaged across 21 days at each age point. Two-way ANOVA, Tukey's post-hoc. *P ≤ 0.05; **P ≤ 0.01; ***P ≤ 0.001; ****P ≤0.0001.

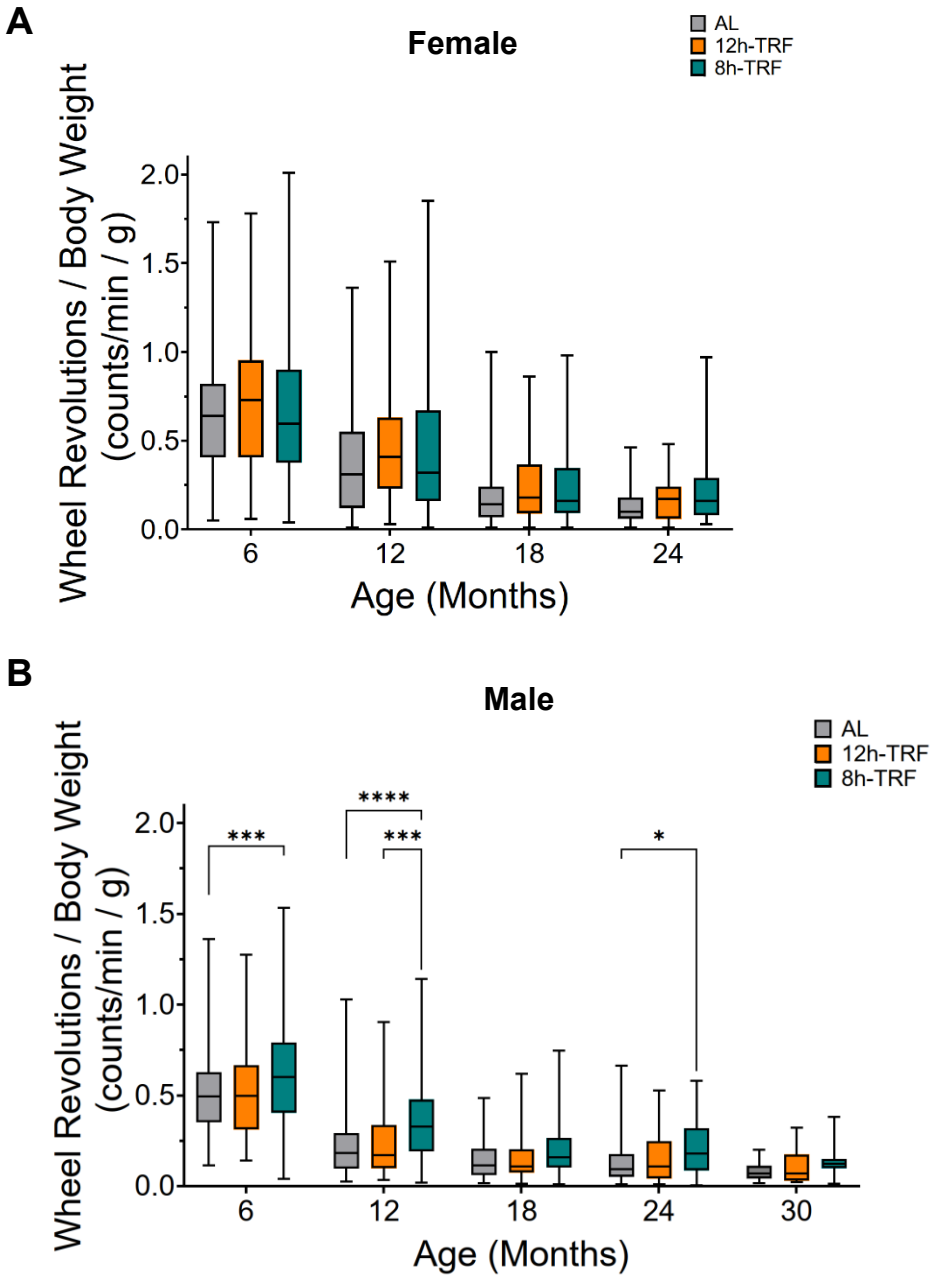

1142 **Figure S5: Wheel activity relative to body weight by monthly age epochs:** (**A**) In females and

1143 (**B**) males, boxplots of wheel revolutions (counts/min) relative to body weight (g) at 6 months of

1144 age and then every 6 months following. Two-way ANOVA, Tukey's post-hoc. *P ≤ 0.05; **P ≤

1145 0.01; ***P ≤ 0.001; ****P ≤0.0001.

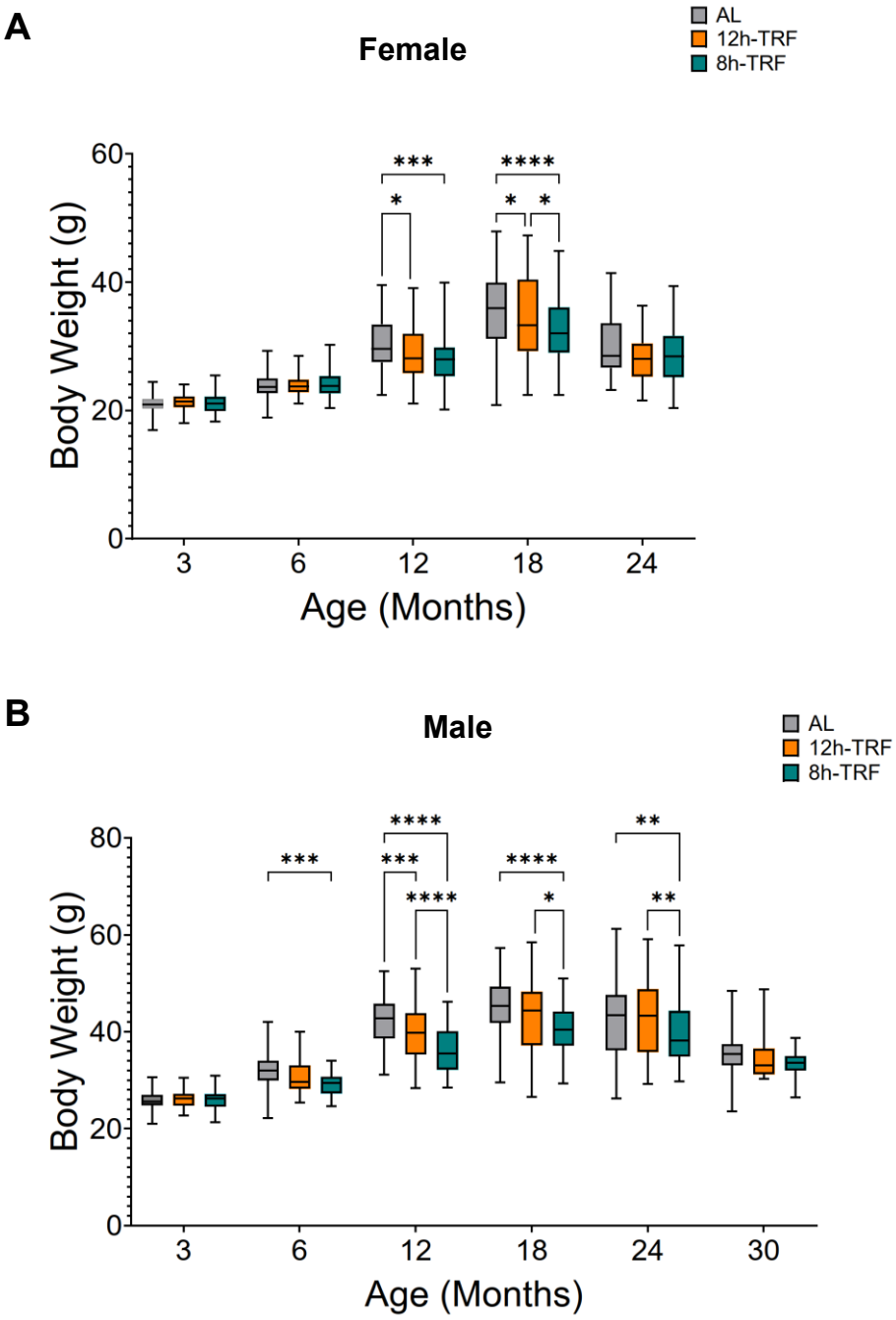

1146 **Figure S6: Body weight by monthly age epochs:** (**A**) In females and (**B**) males, boxplots of body
1147 weight (g) at 3 and 6 months of age and then every 6 months following. Two-way ANOVA,
1148 Tukey's post-hoc. *P ≤ 0.05; **P ≤ 0.01; ***P ≤ 0.001; ****P ≤0.0001.

1149

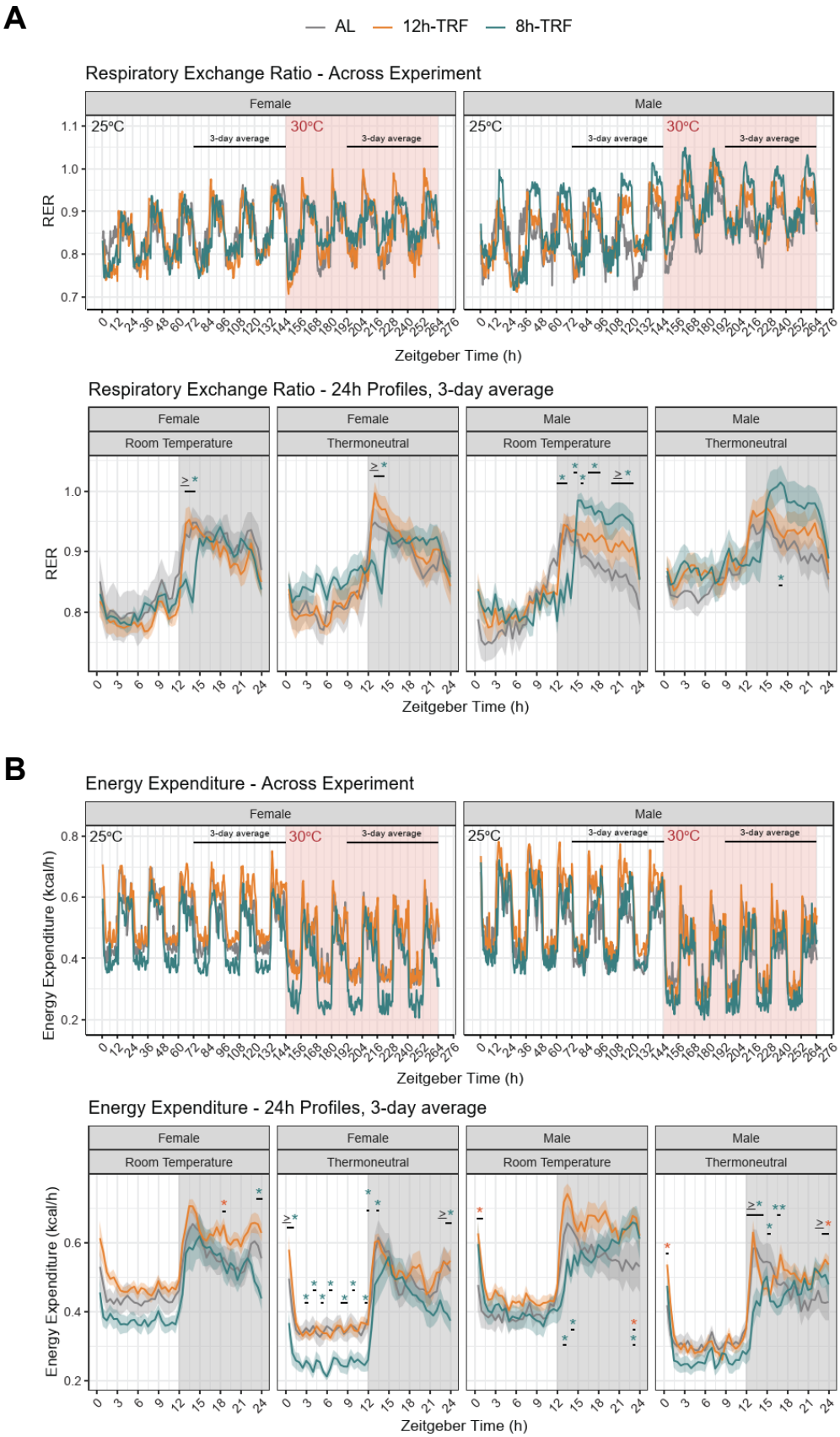
A
AL
12h-TRF
8h-TRF
Respiratory Exchange Ratio - Across Experiment
Female
Male
25°C
30°C
3-day average
RER
Zeitgeber Time (h)
Respiratory Exchange Ratio - 24h Profiles, 3-day average
Room Temperature
Thermoneutral
B
Energy Expenditure - Across Experiment
Energy Expenditure (kcal/h)
Energy Expenditure - 24h Profiles, 3-day average

1150 **Figure S7: Measures of metabolism at 19 months of age in a follow-up cohort of mice:** (**A**)
1151 (*Top*) Respiratory exchange ratios (RER; VCO2/VO2) in females and males throughout a 11-day
1152 recording in Promethion metabolic chambers. 6 days recorded at room temperature (25ºC; white
1153 shaded area), and 5 days were recorded at thermoneutrality (30ºC; red shaded area). (*Bottom*) 24h
1154 profiles of RER averaged from the last 3 days of recording in each temperature. 12h light (white
1155 shaded area), 12h dark (gray shaded area). Means ± SEM (shading) presented in 30-minute bins.
1156 (**B**) (*Top*) Energy expenditure (EE; kcal/h) in females and males throughout the 11-day recording.
1157 6 days recorded at room temperature (25ºC; white shaded area), and 5 days were recorded at
1158 thermoneutrality (30ºC; red shaded area). Measurements are presented in 30-minute bins. (*Bottom*)
1159 24h profiles of EE from the last 3 days of recording in each temperature. 12h light (white shaded
1160 area), 12h dark (gray shaded area). Means ± SEM (shading) presented in 30-minute bins. A and
1161 B: Type III ANOVA (Wald χ^2), and Holm's post-hoc. *P ≤ 0.05; **P ≤ 0.01; ***P ≤ 0.001; ****P
1162 ≤0.0001.

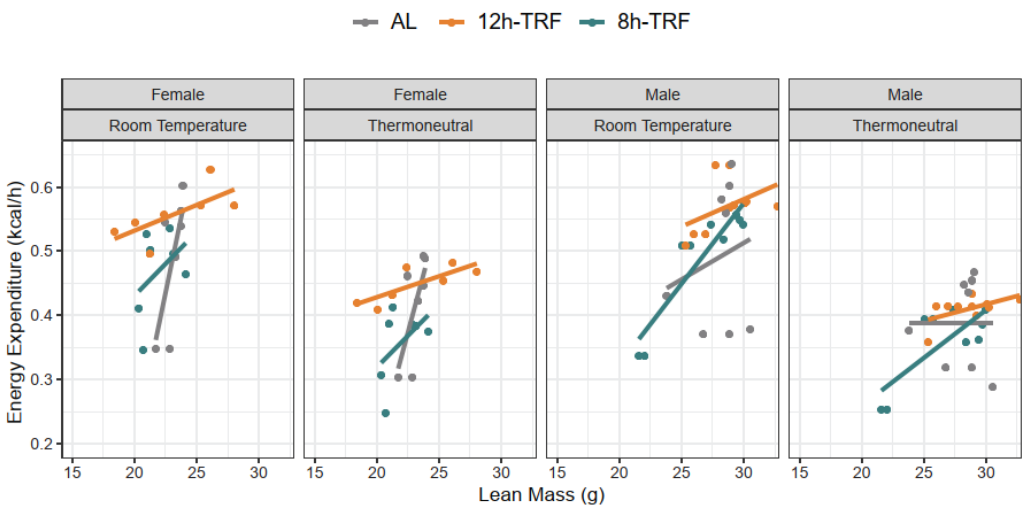

Female Room Temperature						
1. INTERACTION MODEL (Slope Consistency)						
	Df	Sum Sq	Mean Sq	F value	Pr(>F)	signif
Lean	1	0.02322	0.02322	5.97928	0.02729	*
feeding	2	0.02204	0.01102	2.83776	0.09011	ns
Lean:feeding	2	0.02754	0.01377	3.54642	0.0548	ns
Residuals	15	0.05825	0.00388			
2. ANCOVA MODEL (Type III SS)						
	Sum Sq	Df	F value	Pr(>F)	signif	
(Intercept)	0.00554	1	1.09845	0.30928	ns	
Lean	0.01599	1	3.16844	0.09295	ns	
feeding	0.02204	2	2.1836	0.14321	ns	
Residuals	0.08579	17				

Male Room Temperature						
1. INTERACTION MODEL (Slope Consistency)						
	Df	Sum Sq	Mean Sq	F value	Pr(>F)	signif
Lean	1	0.06713	0.06713	12.7309	0.00182	**
feeding	2	0.02161	0.01081	2.04916	0.15383	ns
Lean:feedin	2	0.00929	0.00464	0.88045	0.42935	ns
Residuals	21	0.11074	0.00527			
2. ANCOVA MODEL (Type III SS)						
	Sum Sq	Df	F value	Pr(>F)	signif	
(Intercept)	2.8E-05	1	0.00528	0.94269	ns	
Lean	0.04917	1	9.42346	0.00542	**	
feeding	0.02161	2	2.07069	0.14897	ns	
Residuals	0.12002	23				

Female Thermoneutrality						
1. INTERACTION MODEL (Slope Consistency)						
	Df	Sum Sq	Mean Sq	F value	Pr(>F)	signif
Lean	1	0.02085	0.02085	8.61881	0.01022	*
feeding	2	0.02061	0.0103	4.25862	0.0343	*
Lean:feeding	2	0.01696	0.00848	3.50538	0.05635	ns
Residuals	15	0.03629	0.00242			
2. ANCOVA MODEL (Type III SS)						
	Sum Sq	Df	F value	Pr(>F)	signif	
(Intercept)	0.00416	1	1.32941	0.26487	ns	
Lean	0.01125	1	3.59171	0.0752	ns	
feeding	0.02061	2	3.28915	0.06201	ns	
Residuals	0.05325	17				

Male Thermoneutrality						
1. INTERACTION MODEL (Slope Consistency)						
	Df	Sum Sq	Mean Sq	F value	Pr(>F)	signif
pre_lean	1	0.02215	0.02215	9.1224	0.00651	**
feeding	2	0.00477	0.00239	0.98324	0.39067	ns
pre_lean:fee	2	0.00572	0.00286	1.17758	0.32755	ns
Residuals	21	0.05099	0.00243			
2. ANCOVA MODEL (Type III SS)						
	Sum Sq	Df	F value	Pr(>F)	signif	
(Intercept)	0.00285	1	1.1577	0.2931	ns	
pre_lean	0.01371	1	5.55981	0.02726	*	
feeding	0.00477	2	0.96829	0.39468	ns	
Residuals	0.05671	23				

Figure S8: ANCOVA of TRF effects on energy expenditure: 24h mean EE plotted vs lean mass for females and males. Homogeneity of regression slopes was confirmed for all groups (test of Feeding × Lean Mass interaction, all $p > 0.05$, ns), validating the use of ANCOVA to test for significance of intercepts.

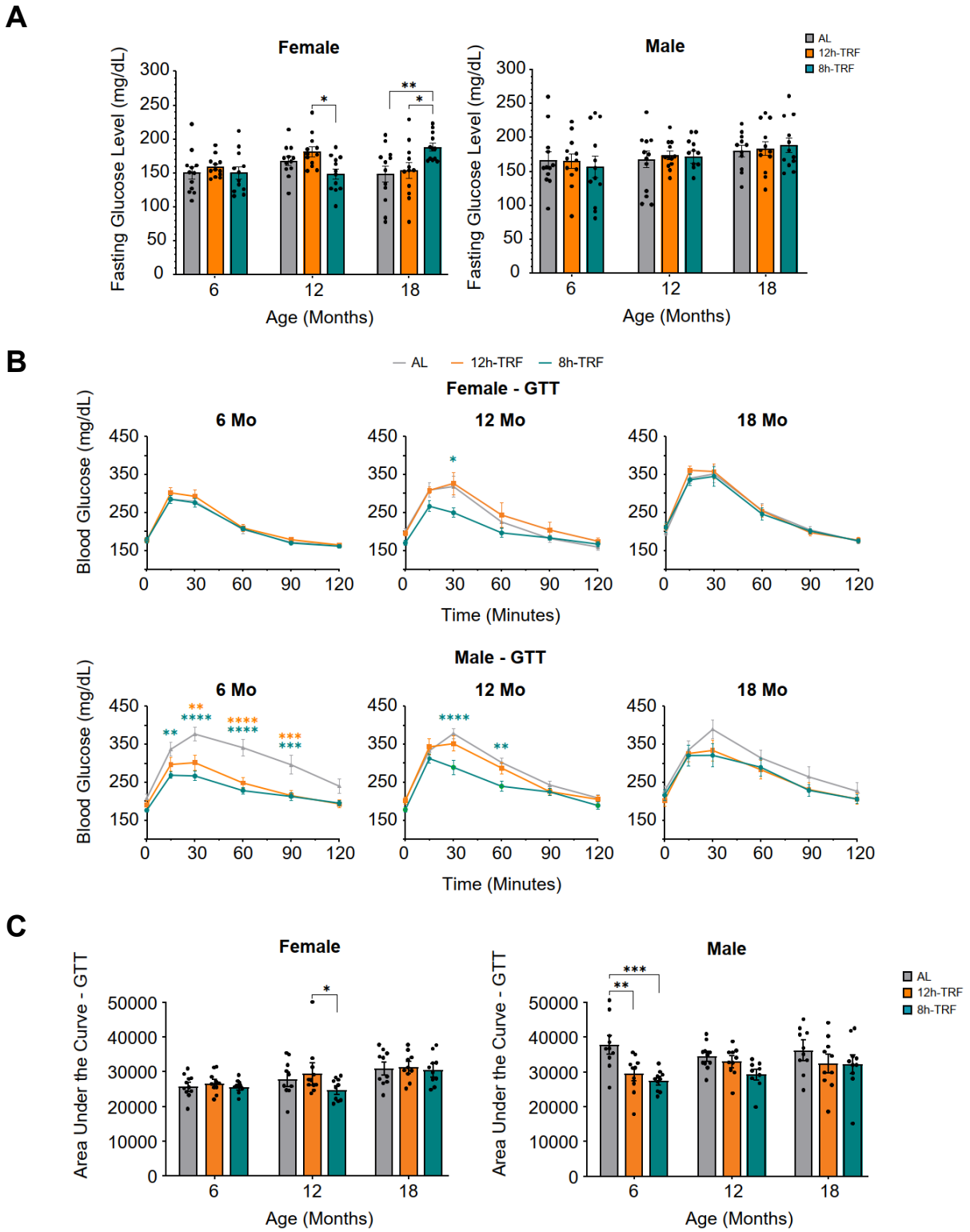

1167 **Figure S9: Fasting glucose levels and glucose tolerance tests in follow-up mouse cohort:** In

1168 females and males: (**A**) Bar graphs of 12h fasting glucose levels (mg/dL) collected at zeitgeber

1169 time (ZT) 10, (**B**) glucose tolerance tests (GTT) performed starting at ZT10, and (**C**) area under
1170 the curve (AUC) for the GTTs tested at 6, 12, and 18 months of age. Means ± SEM (bars). Two-
1171 way ANOVA, Tukey's post-hoc. *P ≤ 0.05; **P ≤ 0.01; ***P ≤ 0.001; ****P ≤0.0001. N=9-12
1172 per group and sex.

1173

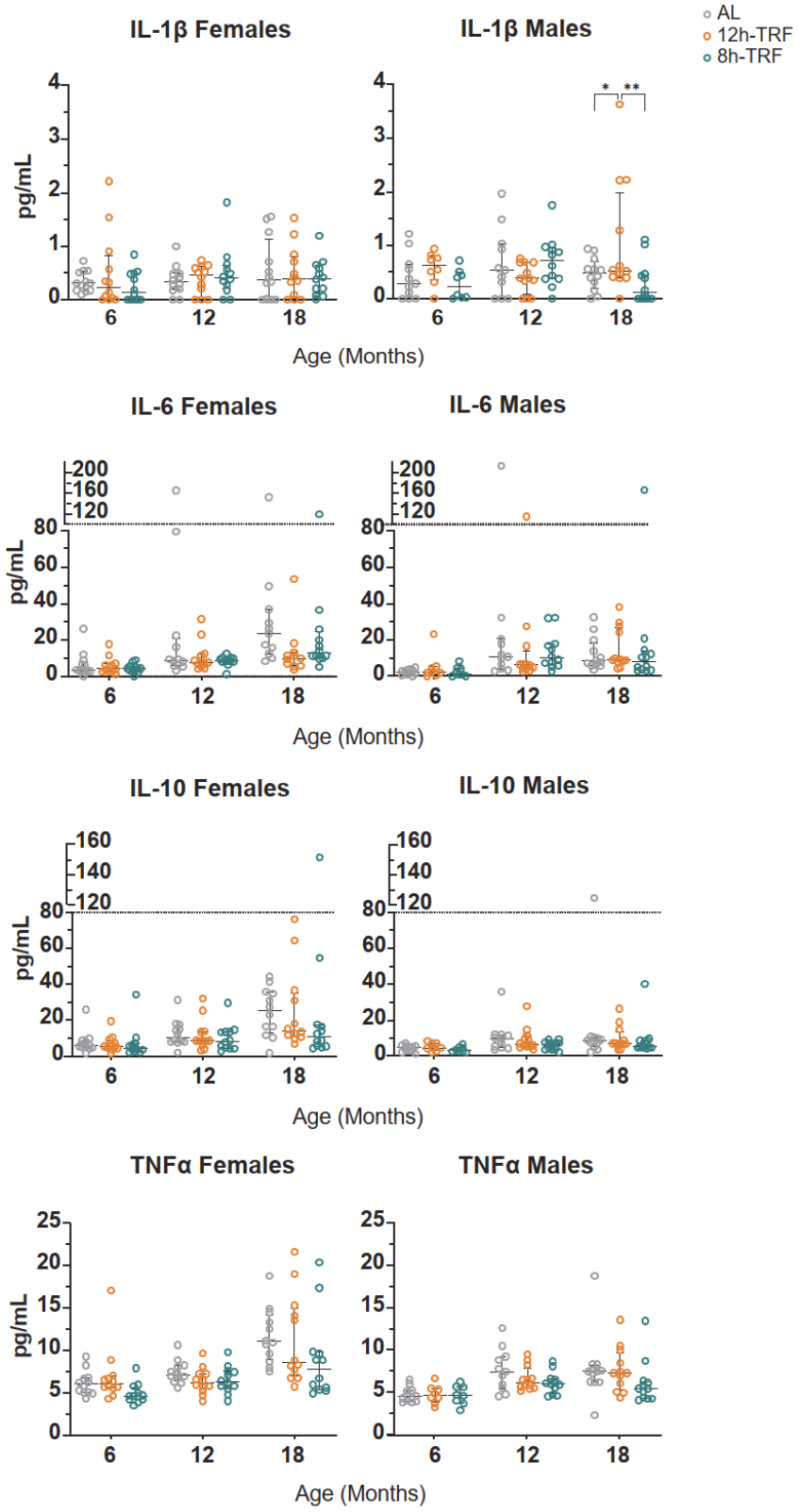
AL
12h-TRF
8h-TRF
IL-1β Females
IL-1β Males
IL-6 Females
IL-6 Males
IL-10 Females
IL-10 Males
TNFα Females
TNFα Males
pg/mL
Age (Months)
6
12
18
*
**

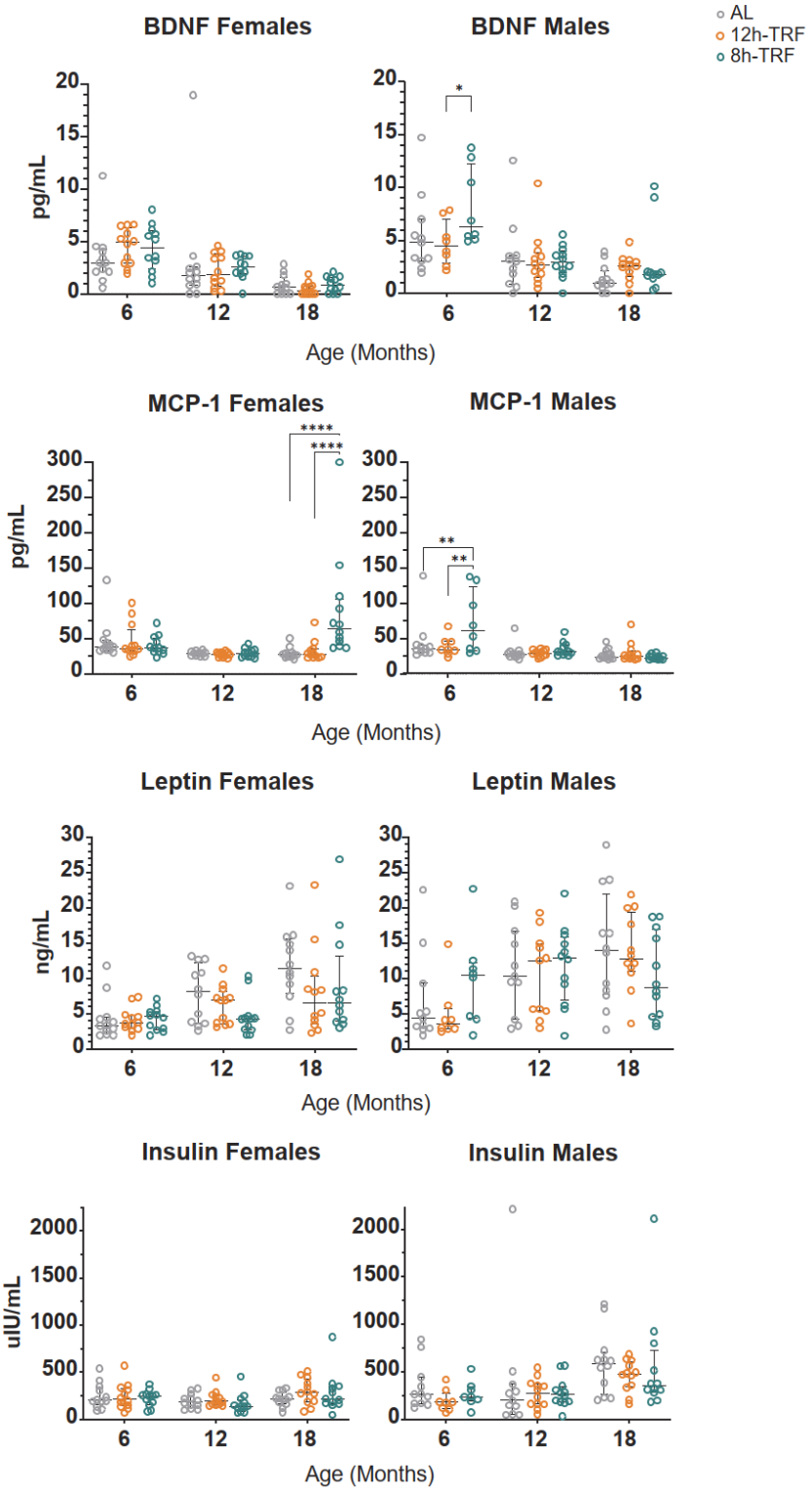

1174 **Figure S10: Circulating levels of adipokines from blood plasma in follow-up mouse cohort.**

1175 In females and males, dot plots of circulating levels of interleukin (IL)-1β, IL-6, IL-10, tumor

1176 necrosis factor α (TNFα), brain-derived neurotrophic factor (BDNF), monocyte chemoattractant
1177 protein (MCP)-1, leptin, and insulin. Plasma was collected at ZT10 from 12h fasted blood at 6, 12,
1178 and 18 months of age. Median with interquartile range. Two-way ANOVA, Tukey's post-hoc. *P
1179 ≤ 0.05; **P ≤ 0.01; ***P ≤ 0.001; ****P ≤0.0001. N=8-12 per group and sex.

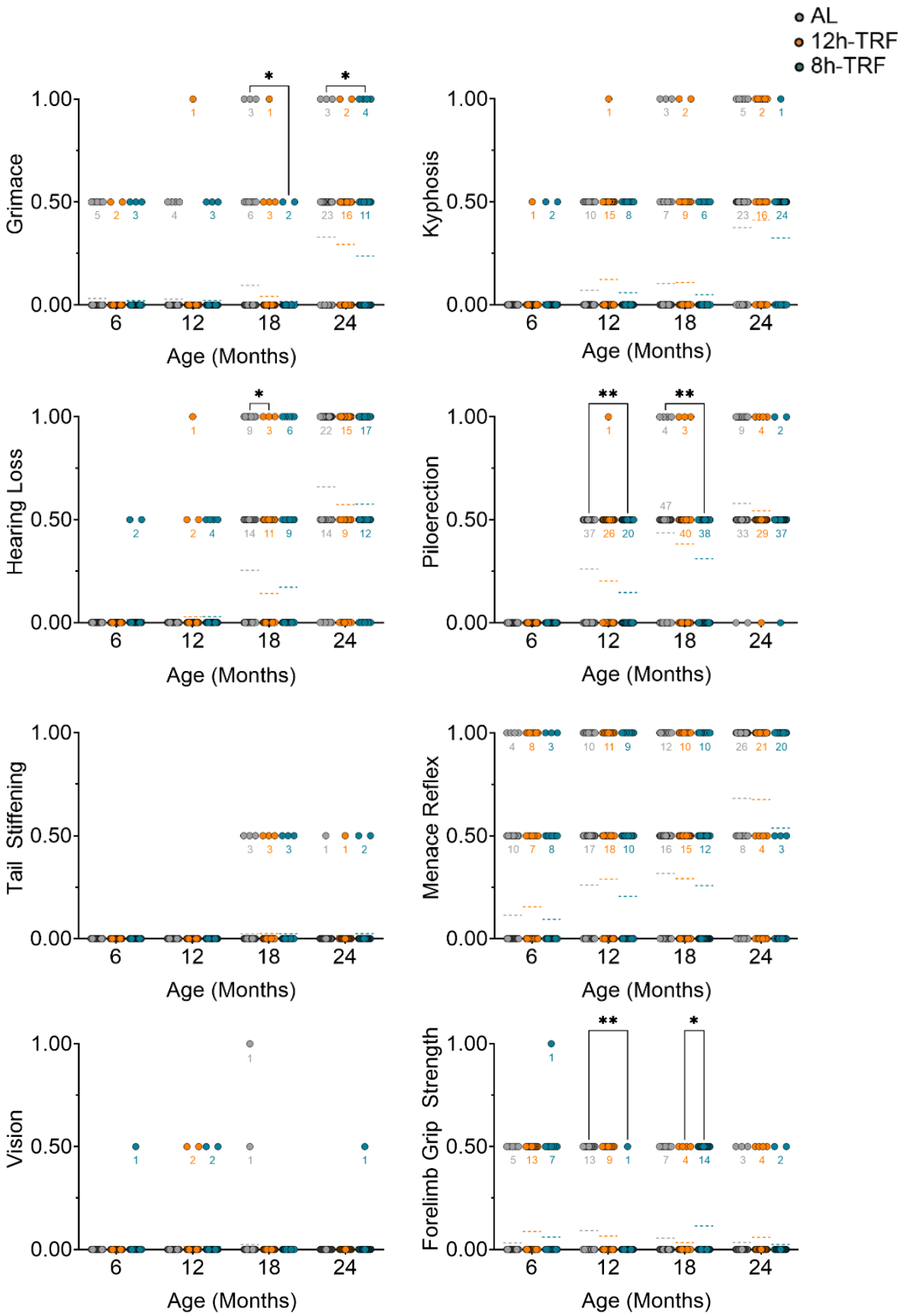
AL
12h-TRF
8h-TRF
Grimace
Kyphosis
Hearing Loss
Piloerection
Tail Stiffening
Menace Reflex
Vision
Forelimb Grip Strength
Age (Months)
1.00
0.50
0.00
6
12
18
24
*
**

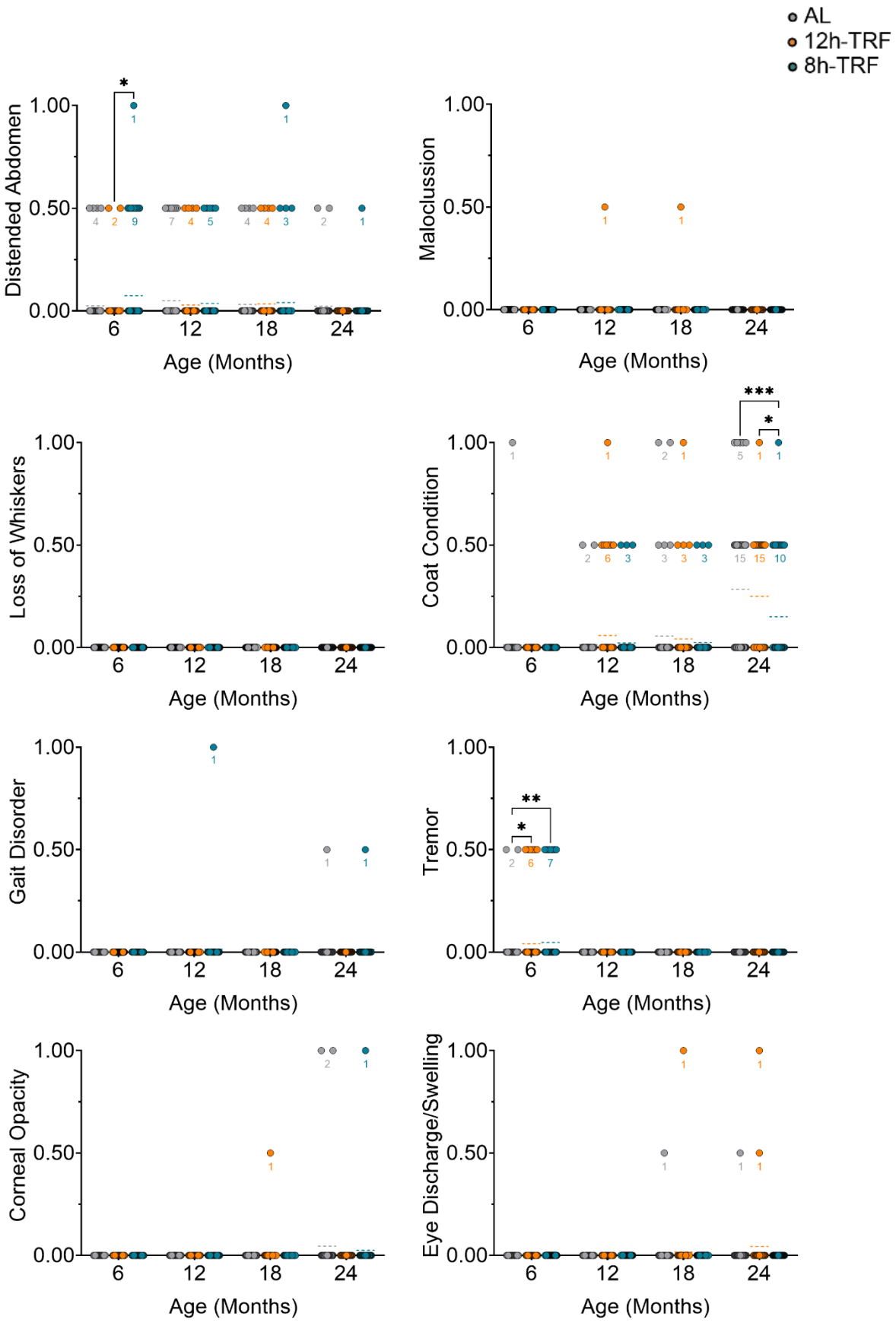
AL
12h-TRF
8h-TRF
Distended Abdomen
Maloclussion
Loss of Whiskers
Coat Condition
Gait Disorder
Tremor
Corneal Opacity
Eye Discharge/Swelling
Age (Months)
1.00
0.50
0.00
6
12
18
24
*
**
***

1181

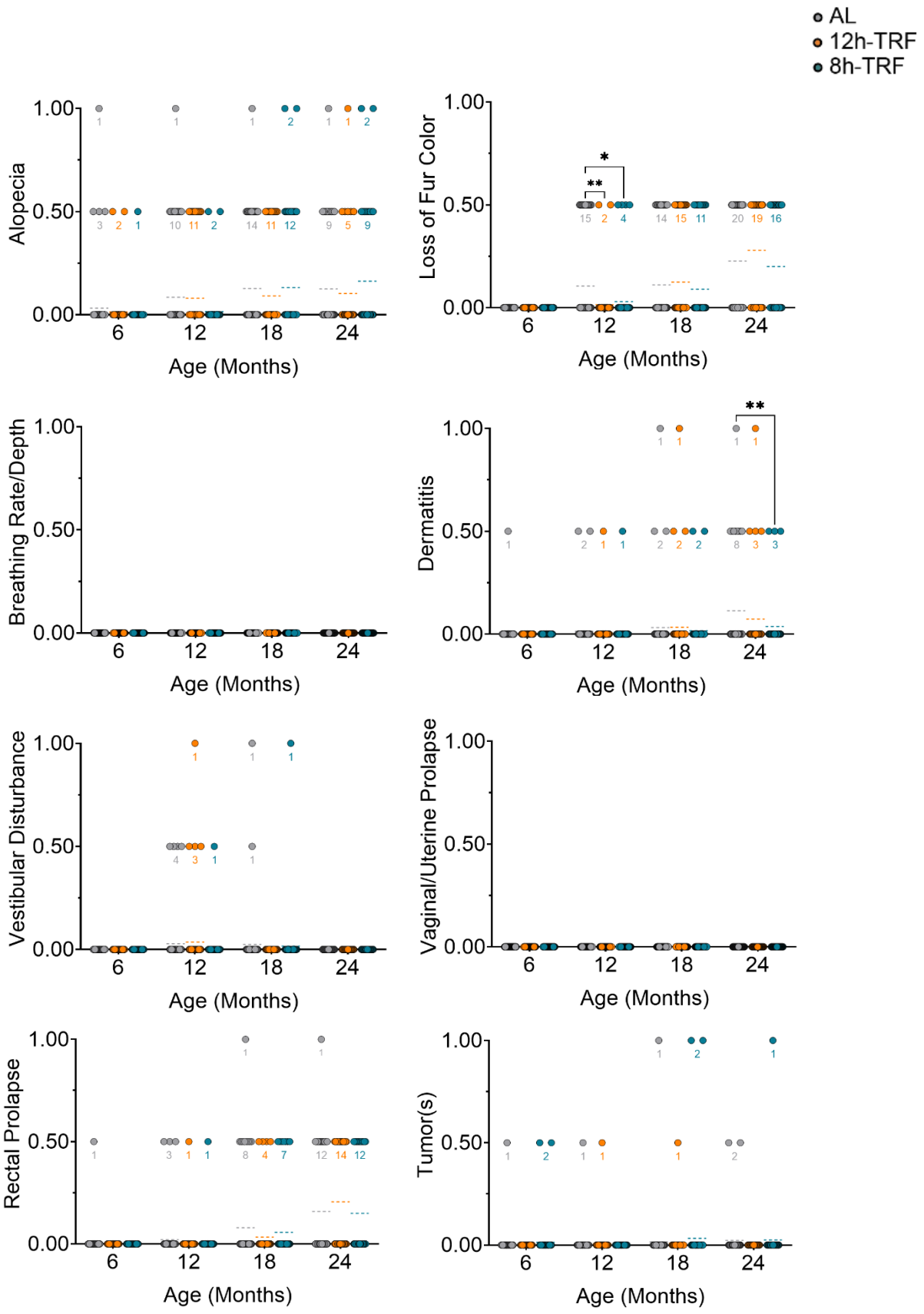
AL
12h-TRF
8h-TRF
Alopecia
Loss of Fur Color
Breathing Rate/Depth
Dermatitis
Vestibular Disturbance
Vaginal/Uterine Prolapse
Rectal Prolapse
Tumor(s)
Age (Months)
1.00
0.50
0.00
6
12
18
24
*
**

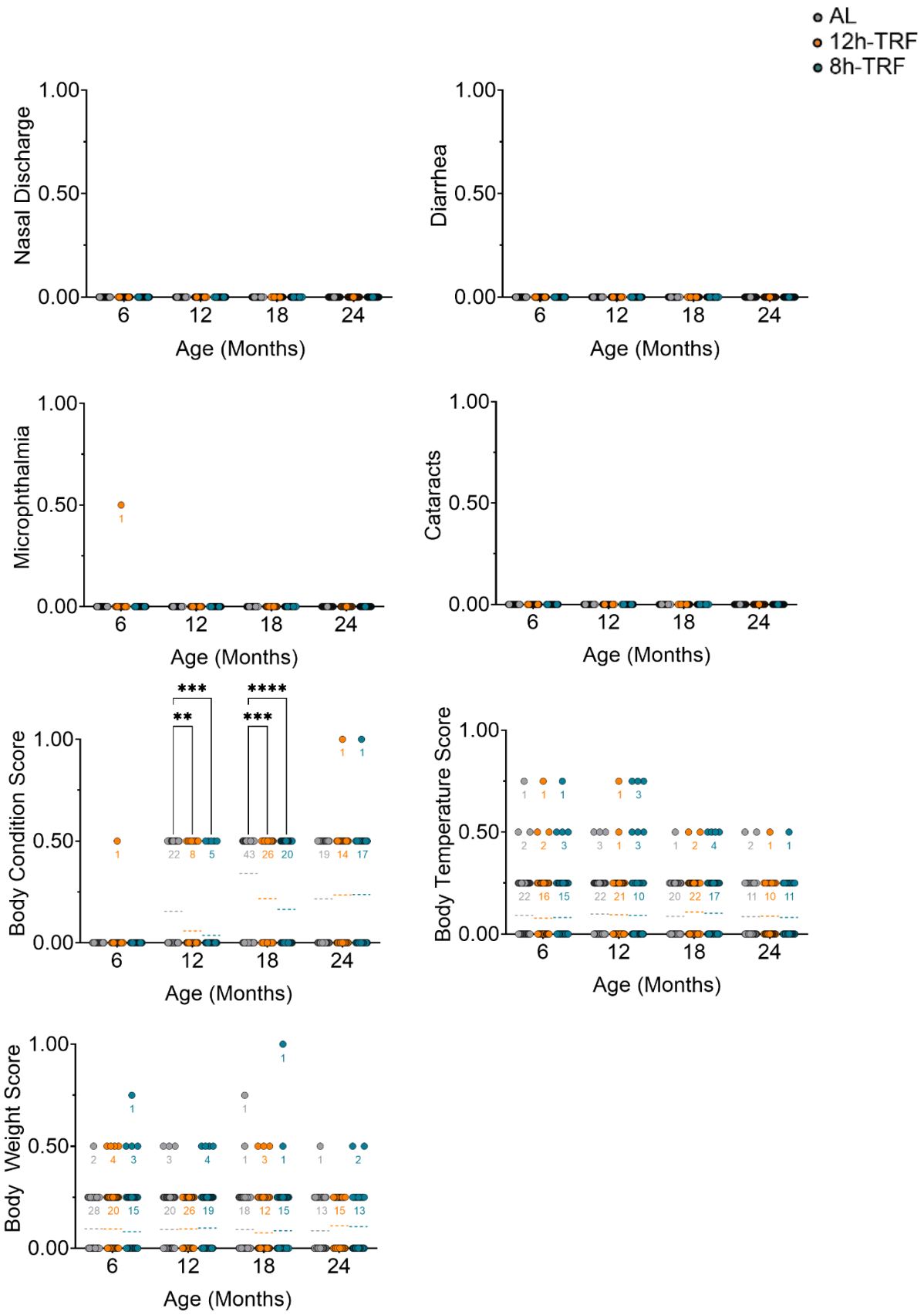
AL
12h-TRF
8h-TRF
Nasal Discharge
Diarrhea
Microphthalmia
Cataracts
Body Condition Score
Body Temperature Score
Body Weight Score
1.00
0.50
0.00
6
12
18
24
Age (Months)
***
**
****
***

1183

Figure S11: Individual frailty parameter scores in females. Dot plots of frailty scores every 6 months of age in females for each of the 31 parameters modified from (*55*). Most parameters scored as 0 for no, 0.5 for mild, and 1 for severe deficit. Body temperature and body weight scores were scored 0, .25, .5, .75, or 1 with higher values representing more severe deviation of the parameter from the group mean. N values shown in graph for any mice with scores >0. Mean shown as dashed line. Two-way ANOVA, Tukey's post-hoc. *P ≤ 0.05; **P ≤ 0.01; ***P ≤ 0.001; ****P ≤0.0001. Total N: AL, N=44-79. 12h-TRF, N=34-74. 8h-TRF, N=40-74.

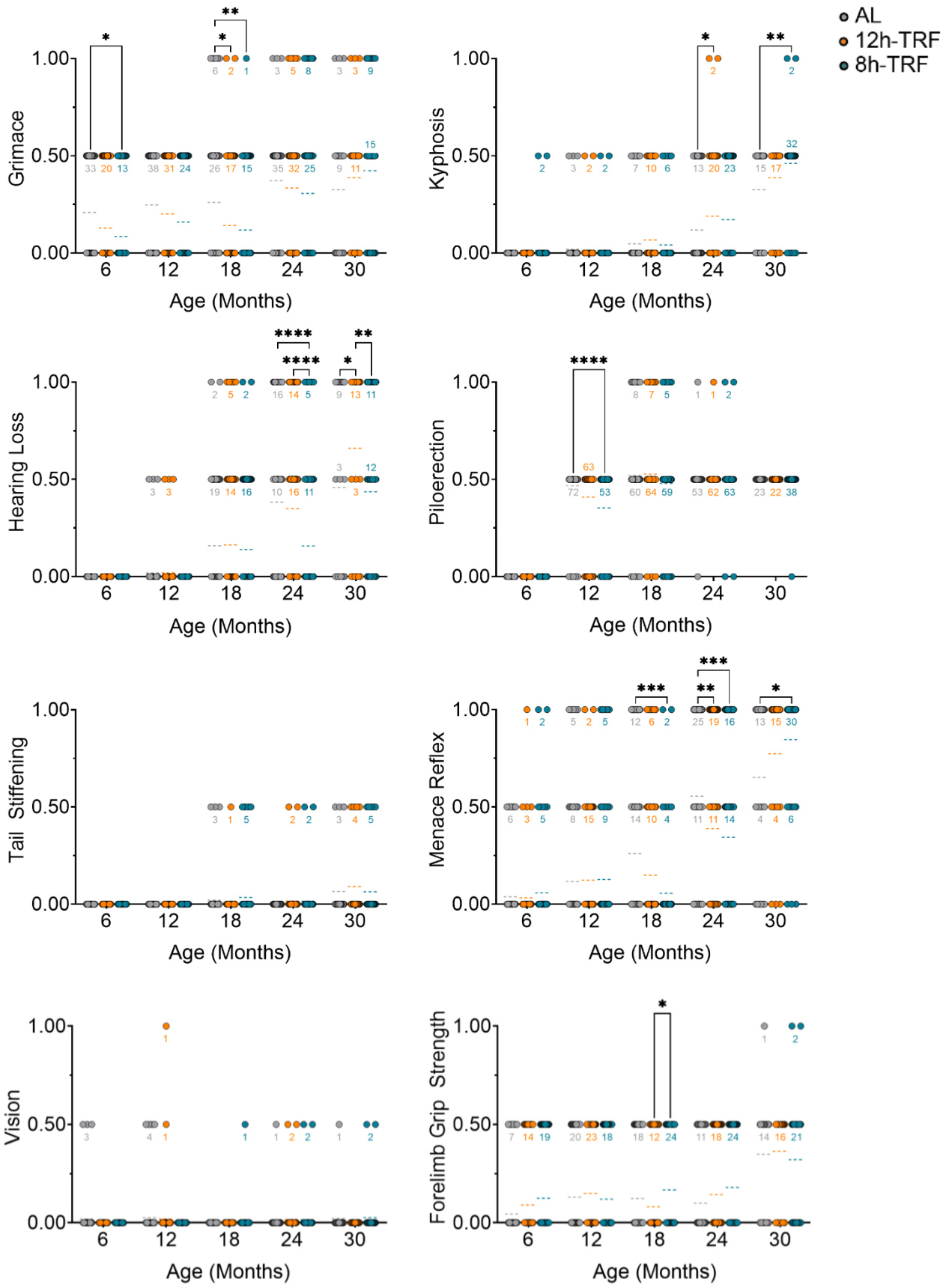
AL
12h-TRF
8h-TRF
Grimace
Kyphosis
Hearing Loss
Piloerection
Tail Stiffening
Menace Reflex
Vision
Forelimb Grip Strength
Age (Months)
1.00
0.50
0.00
6
12
18
24
30

1191

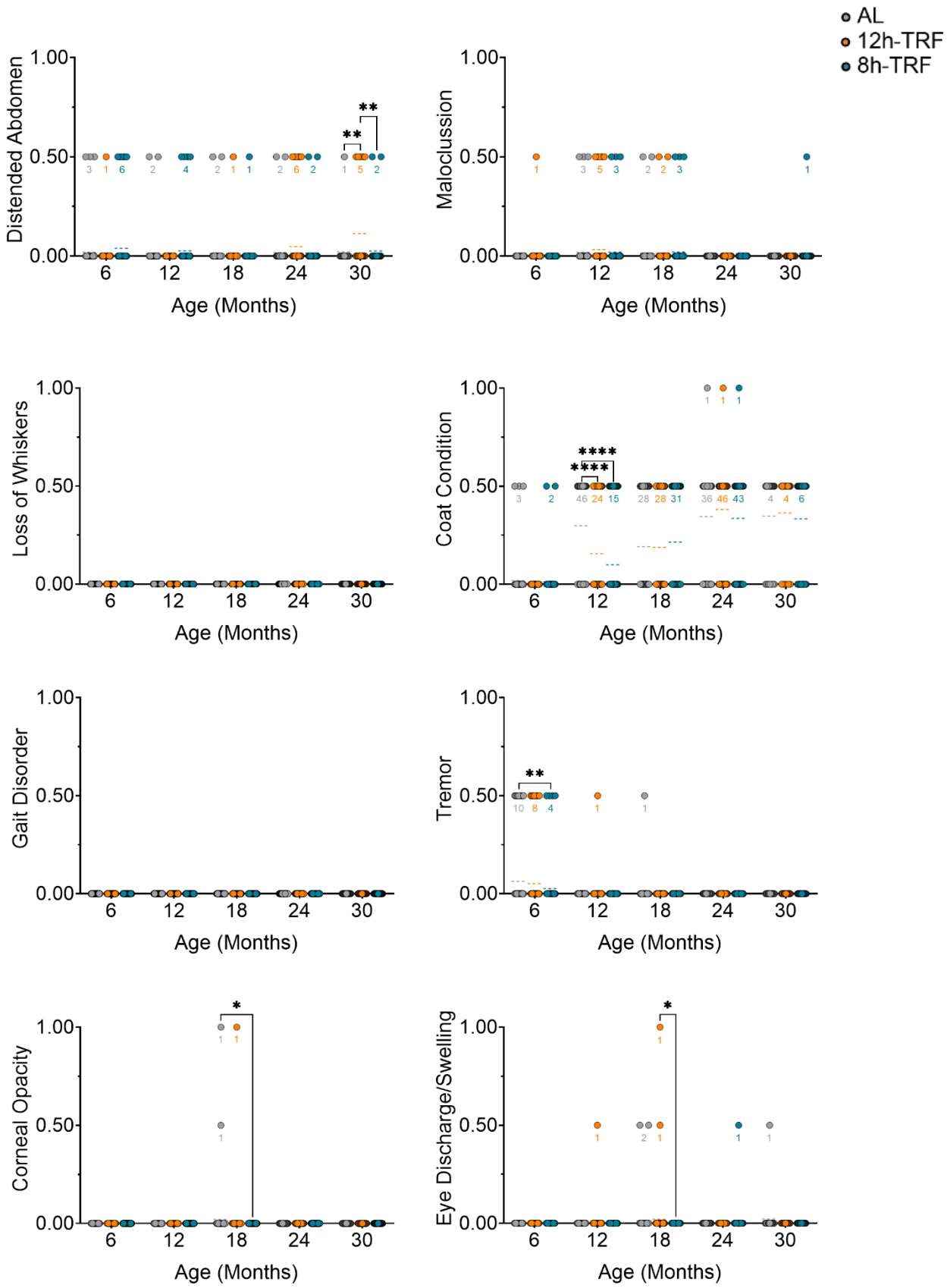
AL
12h-TRF
8h-TRF
Distended Abdomen
Maloclussion
Loss of Whiskers
Coat Condition
Gait Disorder
Tremor
Corneal Opacity
Eye Discharge/Swelling
1.00
0.50
0.00
6
12
18
24
30
Age (Months)
**
****
*

1192

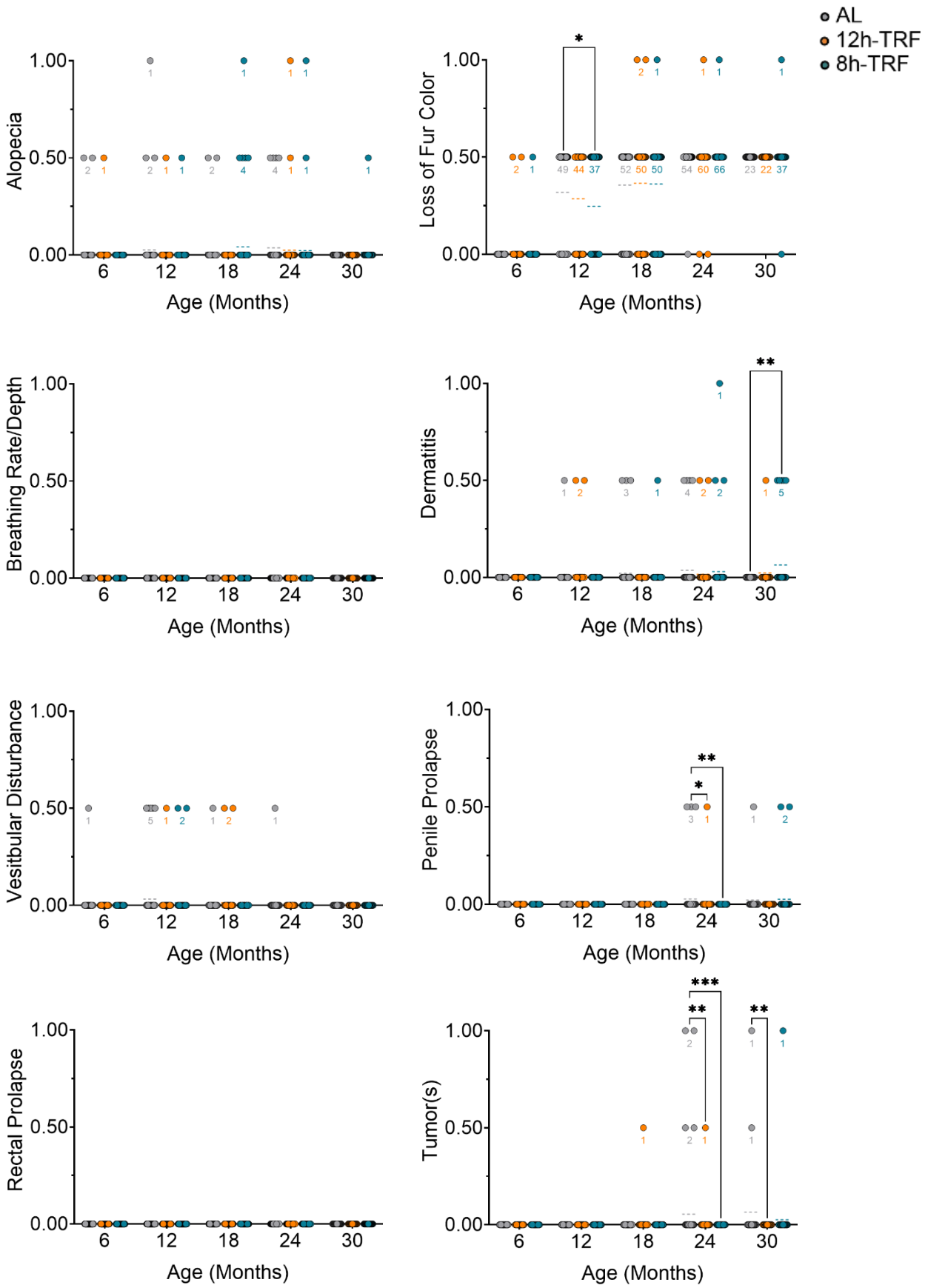
AL
12h-TRF
8h-TRF
Alopecia
Loss of Fur Color
Breathing Rate/Depth
Dermatitis
Vesitbular Disturbance
Penile Prolapse
Rectal Prolapse
Tumor(s)
Age (Months)
1.00
0.50
0.00
6
12
18
24
30
*
**
***

1193

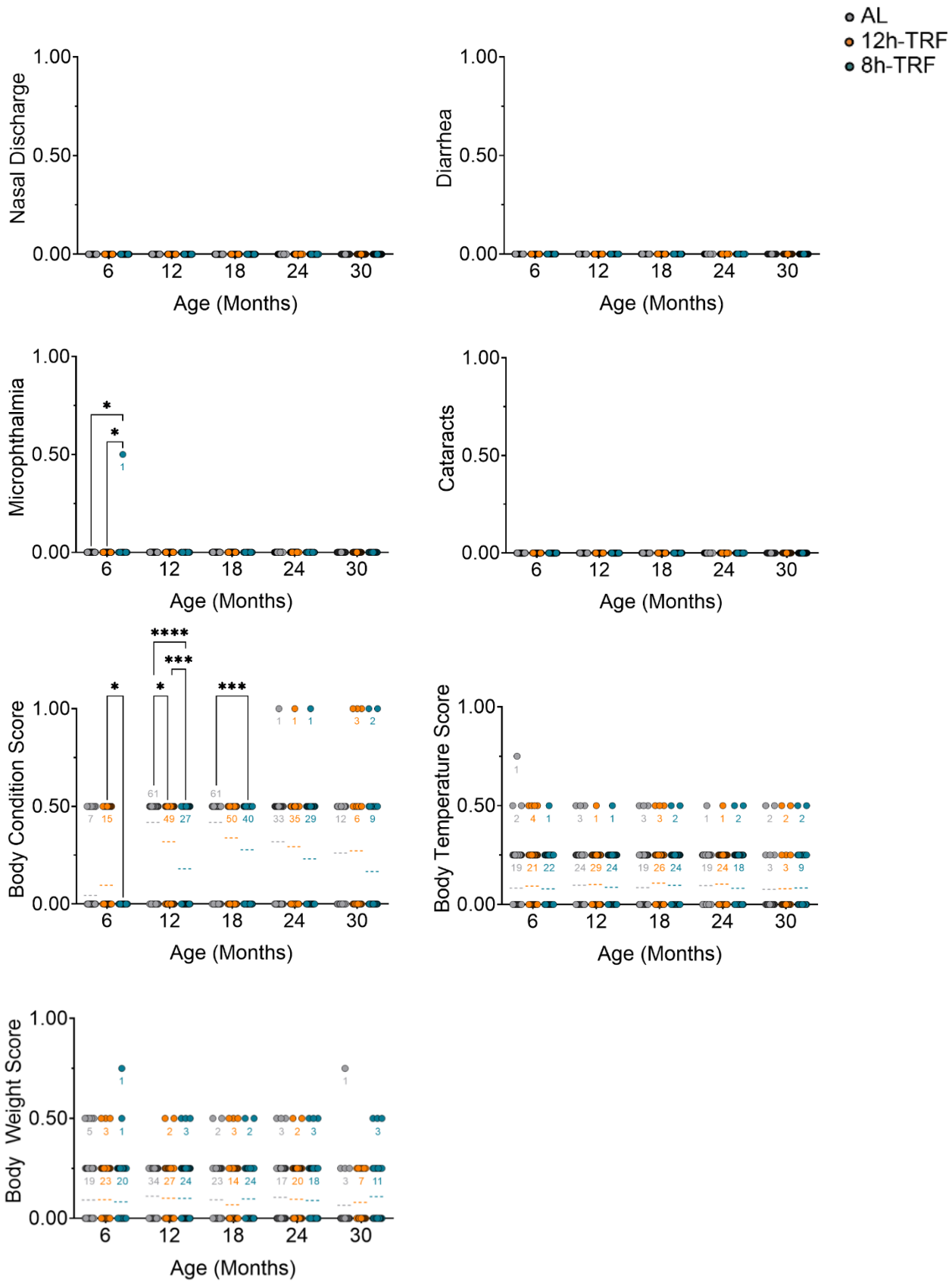
AL
12h-TRF
8h-TRF
Nasal Discharge
Diarrhea
Microphthalmia
Cataracts
Body Condition Score
Body Temperature Score
Body Weight Score
1.00
0.50
0.00
6
12
18
24
30
Age (Months)
*
**
***
****

1194

1195 **Figure S12: Individual frailty parameter scores in males.** Dot plots of frailty scores every 6
1196 months of age in males for each of the 31 parameters modified from (*55*). Most parameters scored
1197 as 0 for no, 0.5 for mild, and 1 for severe deficit. Body temperature and body weight scores were
1198 scored 0, .25, .5, .75, or 1 with higher values representing more severe deviation of the parameter
1199 from the group mean. N values shown in graph for any mice with scores >0. Mean shown as dashed
1200 line. Two-way ANOVA, Tukey's post-hoc. *P ≤ 0.05; **P ≤ 0.01; ***P ≤ 0.001; ****P ≤0.0001.
1201 Total N: AL, N=23-79. 12h-TRF, N=22-78. 8h-TRF, N=39-76.

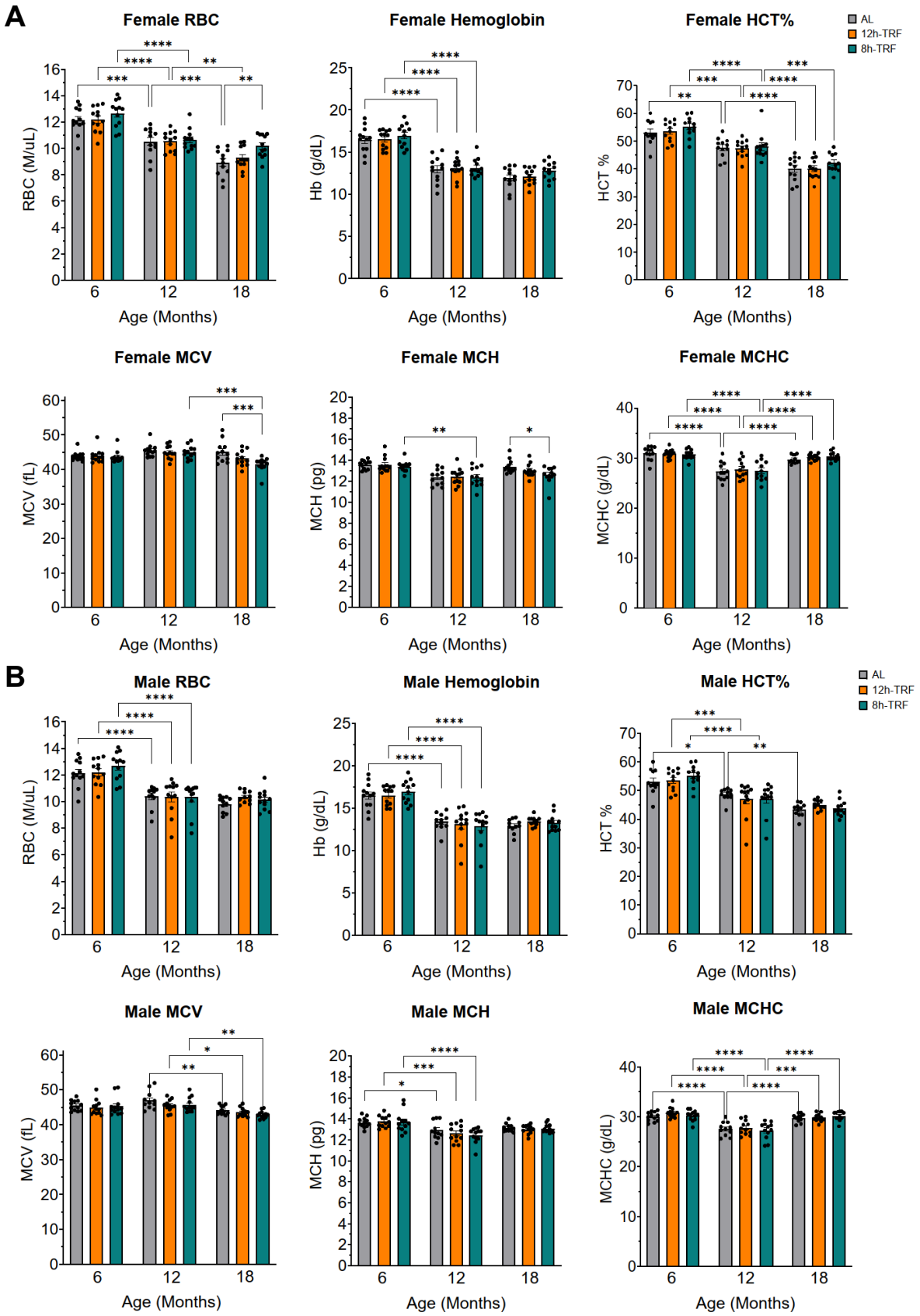

1202 **Figure S13: Red blood cell measures with age in follow-up mouse cohort.** (**A**) In females and

1203 (**B**) males, bar graphs of red blood cell (RBC) counts (M/μL), hemoglobin levels (g/dL),
1204 hematocrit (HCT, percentage of RBCs in total blood volume) (%), mean corpuscular volume
1205 (MCV, average size of RBCs) (fL), mean corpuscular hemoglobin (MCH, average amount of
1206 hemoglobin per RBC) (pg), and mean corpuscular hemoglobin concentration (MCHC, average
1207 concentration of hemoglobin within the volume of the RBC) (g/dL). Measured at ZT10 from 12h
1208 fasted blood at 6, 12, and 18 months of age. Mean ± SEM (bars). Two-way ANOVA, Tukey's
1209 post-hoc. *$P \leq 0.05$; **$P \leq 0.01$; ***$P \leq 0.001$; ****$P \leq 0.0001$. N=11-12 per group and sex.

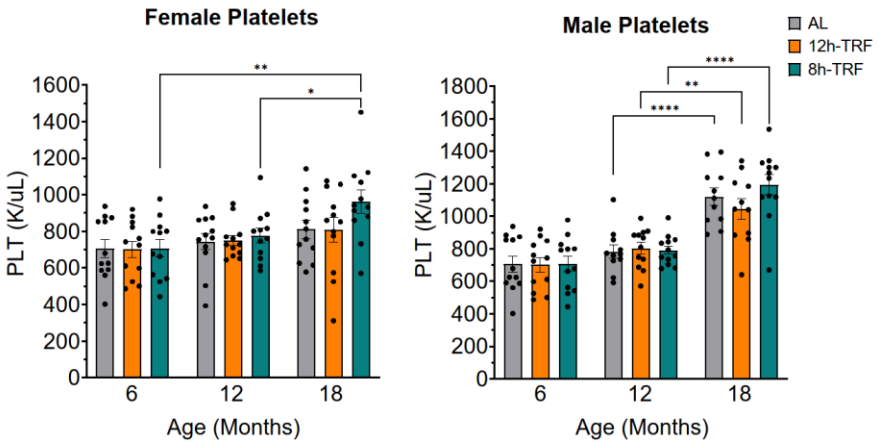

1210 **Figure S14: Platelet counts with age in follow-up mouse cohort.** In females and males,

1211 platelet counts (K/µL). Measured at ZT10 from 12h fasted blood at 6, 12, and 18 months of age.

1212 Mean ± SEM (bars). Two-way ANOVA, Tukey's post-hoc. *P ≤ 0.05; **P ≤ 0.01; ***P ≤ 0.001;

1213 ****P ≤0.0001. N=11-12 per group and sex.

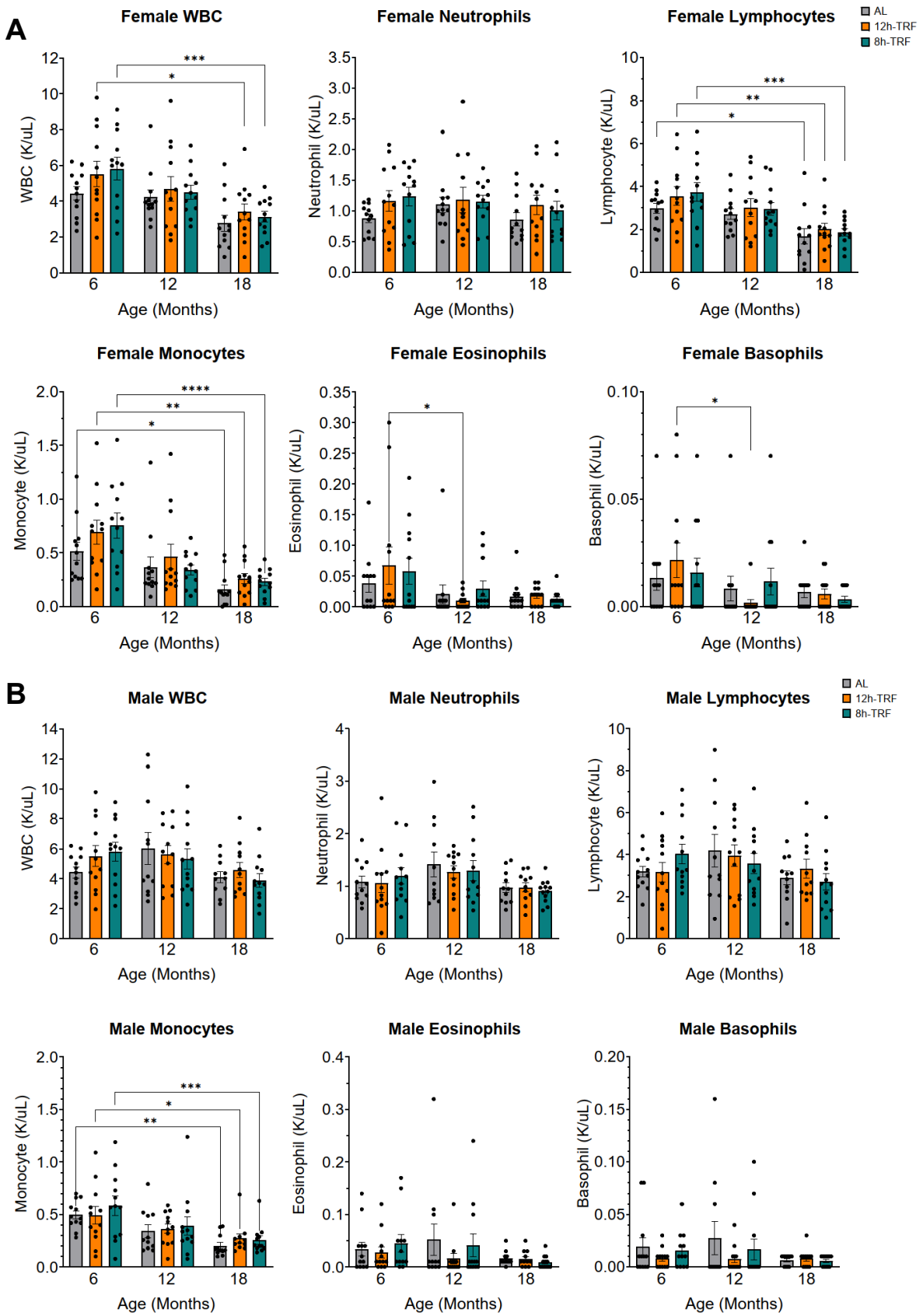

1214 **Figure S15: White blood cells measures with age in follow up mouse cohort.** (**A**) In females

1215 and (**B**) males, bar graphs of total white blood cell (WBC) counts (K/μL) and counts for each

1216 WBC sub-type including neutrophils, lymphocytes, monocytes, eosinophils, and basophils.

1217 Measured at ZT10 from 12h fasted blood at 6, 12, and 18 months of age. Mean ± SEM (bars).

1218 Two-way ANOVA, Tukey's post-hoc. *$P \leq 0.05$; **$P \leq 0.01$; ***$P \leq 0.001$; ****$P \leq 0.0001$.

1219 N=11-12 per group and sex.

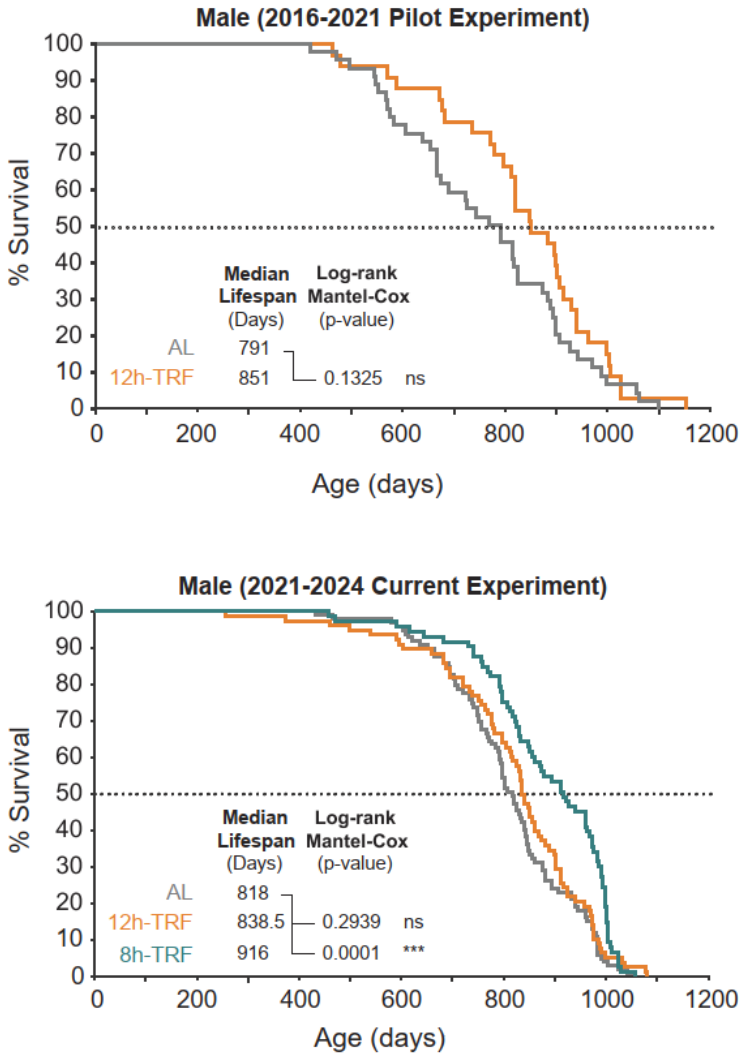

Figure S16: Repeat experiments show 12h-TRF does not extend lifespan in males: Kaplan-Meier survival curves and day median lifespan reached in a pilot experiment vs our current experiment. Log-Rank Mantel-Cox Test for significant difference in overall survival TRF vs AL. Pilot experiment: AL, N=43. 12h-TRF, N=33. Current experiment: AL, N=99. 12h-TRF, N=78. 8h-TRF, N=73.

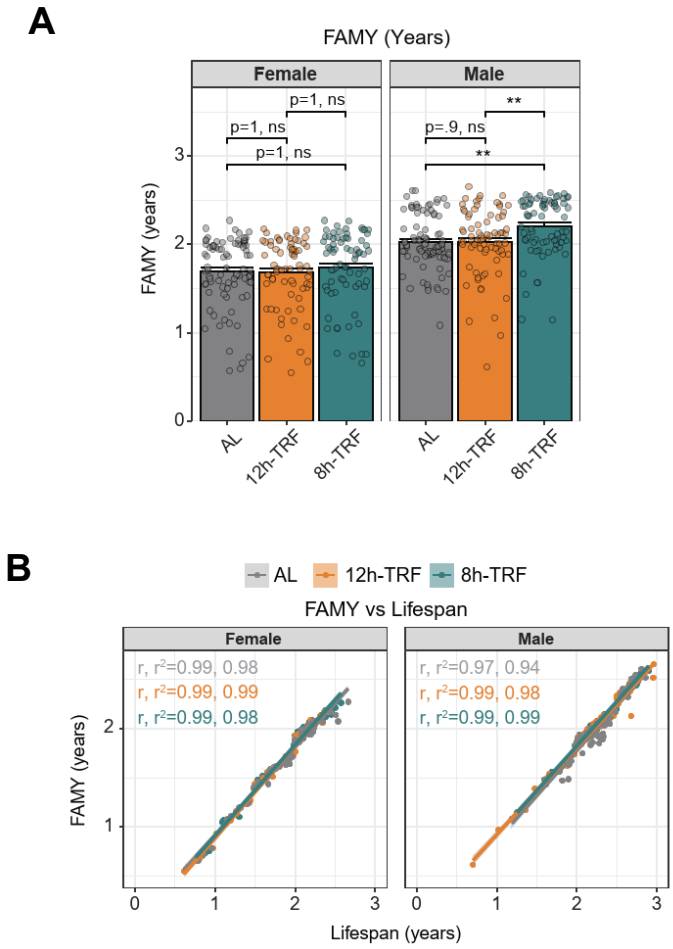

Figure S17: Healthspan as measured by Frailty-Adjusted Mouse Years (FAMY). In females and males: (**A**) FAMY (years) is another method to measure healthspan which utilizes frailty scores as described in (*59*). Higher FAMY = more healthy years. Mean ± SEM (bars). Type III ANOVA, Holm's post-hoc. *P ≤ 0.05; **P ≤ 0.01; ***P ≤ 0.001; ****P ≤0.0001. (**B**) Correlation plots of FAMY vs lifespan in years. Correlation coefficients (r) and coefficients of determination shown (r^2).